

The NRxx Method for Polyatomic Gases

Zhenning Cai*, Ruoli Li†

January 23, 2022

Abstract

In this paper, we propose a numerical regularized moment method to solve the Boltzmann equation with ES-BGK collision term to simulate polyatomic gas flows. This method is an extension to the polyatomic case of the method proposed in [9], which is abbreviated as the NRxx method in [8]. Based on the form of the Maxwellian, the Laguerre polynomials of the internal energy parameter are used in the series expansion of the distribution function. We develop for polyatomic gases all the essential techniques needed in the NRxx method, including the efficient projection algorithm used in the numerical flux calculation, the regularization based on the Maxwellian iteration and the order of magnitude method, and the linearization of the regularization term for convenient numerical implementation. Meanwhile, the particular integrator in time for the ES-BGK collision term is put forward. The shock tube simulations with Knudsen numbers from 0.05 up to 5 are presented to demonstrate the validity of our method. Moreover, the nitrogen shock structure problem is included in our numerical experiments for Mach numbers from 1.53 to 6.1.

Keywords: polyatomic ES-BGK model; moment method; NRxx method

1 Introduction

The kinetic theory has long been playing an important role in the rarefied gas dynamics. As a mesoscopic theory standing between the fluid dynamics and the molecular dynamics, the kinetic theory is built on the basis of the Boltzmann equation, which uses a distribution function to give a statistical description of the distribution of microscopic particles' velocities. In 1940s, Grad [11] proposed the idea using the Hermite expansion to approximate the distribution function, and a 13-moment theory was given in detail in [11]. Recently, based on the idea of Grad, systems with large numbers of moments together with their numerical schemes are considered in [7, 9, 8], where some regularizations inspired by [21, 19] are also taken into account. In [8], the numerical regularized moment method is abbreviated as the NRxx method. However, all these works concentrate only on the monatomic gases, and in this paper, we will develop the NRxx method for the polyatomic case.

The study to apply the moment method to polyatomic gases can be traced back to McCormack [15], where a 17-moment model was proposed. As far as we know, the most recent polyatomic extension of Grad's 13-moment equations is the work of Mallinger [14],

*School of Mathematical Sciences, Peking University, Beijing, China, email: caizn@pku.edu.cn.

†CAPT, LMAM & School of Mathematical Sciences, Peking University, Beijing, China, email: rli@math.pku.edu.cn.

whose system contains only 14 moments. In both models, a great amount of work is devoted to the deduction of the collision terms. In order to generalize the moment theory to large number of moments, we prefer a BGK-like simplified collision operator. As in the monatomic case, the simplest BGK model fails to give correct heat conduction, and for polyatomic gases, it also gives incorrect relaxation collision number, resulting in qualitative errors in temperatures compared with the Boltzmann equation [3]. Possible alternatives include the Rykov model [18] and the ES-BGK model [4], which incorporate physical Prandtl number and relaxation collision number into the collision term. In this work, our investigation is restricted to the ES-BGK model.

For polyatomic gases, besides the velocities of microscopic particles, an additional nonnegative ordinate representing the energy of internal degrees of freedom appears in the distribution function. Thus, in order to expand the distribution function into series, the basis functions are chosen as a combination of Hermite polynomials and Laguerre polynomials with proper translation and scaling based on the macroscopic velocity and translational and rotational temperatures of the gas. By considering the coefficients of the basis functions as moments, a system with infinite number of moment equations is derived. A moment closure is then followed to truncate the system with infinite equations and get a system with only finite equations. The framework for the moment closure is the same as [9]:

1. the Maxwellian iteration is applied to determine the order of magnitude for each moment;
2. by dropping higher order terms, the truncated moments are expressed by moments with lower orders;
3. for easier numerical implementation, the expression is linearized around a Maxwellian.

However, the details of the Maxwellian iteration are significantly different. In the polyatomic case, the iteration is much more complicated than the monatomic case because of the existence of both translational and rotational temperatures in the basis functions, and the process should be conducted carefully. Moreover, for the ES-BGK model, analysis on the moments of the Gauss distribution also increases the complexity. Fortunately, the final result remains a similar form as simple as in [9].

As to the numerical scheme, the general framework in [8] is applicable. A split scheme is applied to divide the transportation part and the collision part, and the transportation part is processed by a finite volume method. Recalling that a special “projection” introduced in [7, 8] is required in the calculation of numerical fluxes, we further develop this technique to the polyatomic case in this paper. Meanwhile, the polyatomic ES-BGK collision term can no longer be solved analytically as the BGK operator [7], and the Crank-Nicolson scheme is applied to ensure the unconditional numerical stability. Our numerical experiments show that our scheme correctly converges to the solution of the Boltzmann equation as the number of moments increases. The distinction between BGK and ES-BGK models, together with the relation between monatomic and polyatomic cases, is illustrated by the numerical results of shock tube problems. Also, we apply the NRxx method to the nitrogen shock structure problem, and the results are comparable to the experimental data.

The rest of this paper is arranged as follows: in Section 2, a brief review of the polyatomic ES-BGK model is given. In Section 3, the polyatomic NRxx method is introduced comprehensively, and in Section 4, a number of numerical experiments are carried out to validate our algorithm. As a summation, some concluding remarks are given in Section 5.

Finally, some involved calculations are collected in the appendix for better readability to the body matter.

2 The ES-BGK Boltzmann equation for polyatomic gases

The ES-BGK model for polyatomic gases, which gives correct Navier-Stokes heat conduction compared with the BGK model, has been deduced in [4, 6]. The polyatomic ES-BGK Boltzmann equation reads

$$\frac{\partial f}{\partial t} + \boldsymbol{\xi} \cdot \nabla_{\mathbf{x}} f = \text{Pr} \cdot \frac{p}{\mu} (G - f), \quad (2.1)$$

where f denotes the molecule distribution, which is a positive function $f = f(t, \mathbf{x}, \boldsymbol{\xi}, I)$ with $\mathbf{x}, \boldsymbol{\xi} \in \mathbb{R}^3$ and $t, I \in \mathbb{R}^+$. The parameters t, \mathbf{x} and $\boldsymbol{\xi}$ stand for the time, spatial position and microscopic molecule velocity respectively, and I is an internal energy parameter. In the right hand side of (2.1), Pr is the Prandtl number, p is the pressure, and μ denotes the viscosity coefficient. G is a generalized Gaussian defined as

$$G(t, \mathbf{x}, \boldsymbol{\xi}, I) = \frac{\rho \Lambda_{\delta}}{\sqrt{\det(2\pi\mathcal{T})} (RT_{\text{rel}})^{\delta/2}} \exp \left(-\frac{1}{2} (\boldsymbol{\xi} - \mathbf{u})^T \mathcal{T}^{-1} (\boldsymbol{\xi} - \mathbf{u}) - \frac{I^{2/\delta}}{RT_{\text{rel}}} \right). \quad (2.2)$$

Here δ is the total number of molecular internal degrees of freedom, and R is the gas constant. The density ρ and the macroscopic velocity \mathbf{u} are related to the distribution function f through

$$\rho = \int_{\mathbb{R}^3 \times \mathbb{R}^+} f \, d\boldsymbol{\xi} \, dI, \quad \mathbf{u} = \frac{1}{\rho} \int_{\mathbb{R}^3 \times \mathbb{R}^+} \boldsymbol{\xi} f \, d\boldsymbol{\xi} \, dI, \quad (2.3)$$

and T_{rel} is a relaxation temperature

$$T_{\text{rel}} = Z^{-1} T_{\text{eq}} + (1 - Z^{-1}) T_{\text{int}}, \quad (2.4)$$

where Z is the relaxation collision number. For polyatomic gases, three temperatures are used frequently, including the translational temperature T_{tr} , the internal temperature T_{int} , and the equilibrium temperature T_{eq} . They are defined by

$$T_{\text{tr}} = \frac{1}{3\rho R} \int_{\mathbb{R}^3 \times \mathbb{R}^+} |\boldsymbol{\xi} - \mathbf{u}|^2 f \, d\boldsymbol{\xi} \, dI, \quad (2.5)$$

$$T_{\text{int}} = \frac{2}{\delta \rho R} \int_{\mathbb{R}^3 \times \mathbb{R}^+} I^{2/\delta} f \, d\boldsymbol{\xi} \, dI, \quad (2.6)$$

$$T_{\text{eq}} = (3T_{\text{tr}} + \delta T_{\text{int}}) / (3 + \delta). \quad (2.7)$$

And the pressure p is obtained from the ideal gas law:

$$p = \rho R T_{\text{eq}}. \quad (2.8)$$

Now it only remains to define Λ_{δ} and \mathcal{T} :

$$\Lambda_{\delta} = \left[\int_{\mathbb{R}^+} e^{-I^{2/\delta}} \, dI \right]^{-1}, \quad \mathcal{T} = (1 - Z^{-1}) [(1 - \nu) R T_{\text{tr}} \text{Id} + \nu \Theta / \rho] + Z^{-1} R T_{\text{eq}} \text{Id}, \quad (2.9)$$

where

$$\Theta = \int_{\mathbb{R}^3 \times \mathbb{R}^+} (\boldsymbol{\xi} - \mathbf{u}) \otimes (\boldsymbol{\xi} - \mathbf{u}) f \, d\boldsymbol{\xi} \, dI, \quad \nu = \frac{1 - \text{Pr}^{-1}}{1 - Z^{-1}}, \quad (2.10)$$

and Id stands for the identity matrix.

3 The NRxx method for polyatomic ES-BGK equation

In this section, we are going to extend the NRxx method proposed in [7, 9] to the polyatomic case, which includes the following steps:

1. The distribution function is expanded into a series with specially selected basis functions.
2. A system with infinite number of moment equations is deduced.
3. The moment system is truncated at a certain place and made closed by regularization.
4. The regularization term is linearized in order to simplify the numerical implementation.
5. The numerical method is carried out following [8].

The details are introduced in the following five subsections.

3.1 Spectral representation of the velocity space

In the NRxx method for the monatomic gases, the Hermite polynomials have been employed to construct the basis functions of the velocity space, since Hermite polynomials are orthogonal over the region $(-\infty, +\infty)$. For the polyatomic distribution function, since $I \in \mathbb{R}^+$, we use the Laguerre polynomials, which are orthogonal over the region $[0, +\infty)$, as the basis functions in the ordinate I . Thus the basis function has the following form:

$$\begin{aligned} \psi_{\alpha,k,T_{\text{tr}},T_{\text{int}}}(\mathbf{v}, J) &= \frac{2}{\delta} \left(\gamma_k^{(m)} \right)^{-1} (RT_{\text{int}})^{-(\delta/2+k)} L_k^{(m)}(J) \exp(-J) \cdot \\ &\quad \left(\sqrt{2\pi} \right)^{-3} (RT_{\text{tr}})^{-\frac{|\alpha|+3}{2}} \prod_{d=1}^3 He_{\alpha_d}(v_d) \exp\left(-\frac{v_d^2}{2}\right), \end{aligned} \quad (3.1)$$

where $\alpha = (\alpha_1, \alpha_2, \alpha_3)$ is a multi-index, and

$$m = \delta/2 - 1, \quad \gamma_k^{(m)} = \frac{\Gamma(m+k+1)}{\Gamma(k+1)}, \quad (3.2)$$

$$L_k^{(m)}(J) = \frac{J^{-m} e^J}{k!} \frac{d^k}{dJ^k} (e^{-J} J^{k+m}), \quad (3.3)$$

$$He_n(x) = (-1)^n \exp\left(\frac{x^2}{2}\right) \frac{d^n}{dx^n} \exp\left(-\frac{x^2}{2}\right). \quad (3.4)$$

Some properties of the Laguerre polynomials $L_k^{(m)}$ and the Hermite polynomials He_n can be found in Appendix A. With equation (3.1), the distribution function $f(\boldsymbol{\xi}, I)$ is expanded as

$$f(\boldsymbol{\xi}, I) = \sum_{\alpha \in \mathbb{N}^3} \sum_{k \in \mathbb{N}} f_{\alpha,k} \psi_{\alpha,k,T_{\text{tr}},T_{\text{int}}} \left(\frac{\boldsymbol{\xi} - \mathbf{u}}{\sqrt{RT_{\text{tr}}}}, \frac{I^{2/\delta}}{RT_{\text{int}}} \right). \quad (3.5)$$

Let us consider the general case when T_{tr} , T_{int} and \mathbf{u} have no relation with the distribution function f . Using the orthogonality of the Laguerre and Hermite polynomials, we can

deduce that

$$\int_{\mathbb{R}^3 \times \mathbb{R}^+} f \, d\boldsymbol{\xi} \, dI = f_{0,0}, \quad (3.6a)$$

$$\int_{\mathbb{R}^3 \times \mathbb{R}^+} \xi_j f \, d\boldsymbol{\xi} \, dI = f_{0,0} u_j + f_{e_j,0}, \quad j = 1, 2, 3, \quad (3.6b)$$

$$\int_{\mathbb{R}^3 \times \mathbb{R}^+} I^{2/\delta} f \, d\boldsymbol{\xi} \, dI = \frac{1}{2} \delta R T_{\text{int}} f_{0,0} - f_{0,1}, \quad (3.6c)$$

$$\int_{\mathbb{R}^3 \times \mathbb{R}^+} \frac{1}{2} |\boldsymbol{\xi}|^2 f \, d\boldsymbol{\xi} \, dI = \frac{1}{2} f_{0,0} |\mathbf{u}|^2 + \sum_{j=1}^3 \left(\frac{1}{2} R T_{\text{tr}} f_{0,0} + u_j f_{e_j,0} + f_{2e_j,0} \right). \quad (3.6d)$$

If \mathbf{u} is the macroscopic velocity and T_{tr} , T_{int} are the translational and internal temperatures for the distribution f , using (2.3), (2.5), (2.6) and (3.6), we conclude

$$f_{0,0} = \rho, \quad f_{e_j,0} = f_{0,1} = \sum_{d=1}^3 f_{2e_d,0} = 0, \quad j = 1, 2, 3. \quad (3.7)$$

If (3.7) is satisfied, then (3.5) is called as a *normal representation* of f . If (3.5) is not a normal representation, then the density, momentum and translational and internal energies can be easily calculated through (3.6). For a normal representation, we have

$$\Theta_{ij} = (1 + \delta_{ij}) f_{e_i+e_j,0} + \delta_{ij} \rho R T_{\text{tr}}, \quad i, j = 1, 2, 3. \quad (3.8)$$

where Θ is defined in (2.10).

3.2 The moment equations for the ES-BGK model

In this section, we are going to derive equations for the moment set $\{f_{\alpha,k}\}$. The general strategy is to substitute (3.5) into (2.1), and then match the coefficients of the same basis functions. For the left hand side of (3.5), the process is similar as that in [9], and the detailed derivation can be found in Appendix B. Suppose G has the following expansion:

$$G(t, \mathbf{x}, \boldsymbol{\xi}, I) = \sum_{\alpha \in \mathbb{N}^3} \sum_{k \in \mathbb{N}} G_{\alpha,k}(t, \mathbf{x}) \psi_{\alpha,k,T_{\text{tr}},T_{\text{int}}} \left(\frac{\boldsymbol{\xi} - \mathbf{u}}{\sqrt{R T_{\text{tr}}}}, \frac{I^{2/\delta}}{R T_{\text{int}}} \right), \quad (3.9)$$

Then the analytical expressions of the moment equations are obtained as

$$\begin{aligned} & \frac{\partial f_{\alpha,k}}{\partial t} + \sum_{d=1}^3 \frac{\partial u_d}{\partial t} f_{\alpha-e_d,k} + \frac{1}{2} \frac{\partial(R T_{\text{tr}})}{\partial t} \sum_{d=1}^3 f_{\alpha-2e_d,k} - (m+k) \frac{\partial(R T_{\text{int}})}{\partial t} f_{\alpha,k-1} \\ & + \sum_{j=1}^3 \left[\left(R T_{\text{tr}} \frac{\partial f_{\alpha-e_j,k}}{\partial x_j} + u_j \frac{\partial f_{\alpha,k}}{\partial x_j} + (\alpha_j + 1) \frac{\partial f_{\alpha+e_j,k}}{\partial x_j} \right) \right. \\ & + \sum_{d=1}^3 \frac{\partial u_d}{\partial x_j} (R T_{\text{tr}} f_{\alpha-e_d-e_j,k} + u_j f_{\alpha-e_d,k} + (\alpha_j + 1) f_{\alpha-e_d+e_j,k}) \\ & + \frac{1}{2} \frac{\partial(R T_{\text{tr}})}{\partial x_j} \sum_{d=1}^3 (R T_{\text{tr}} f_{\alpha-2e_d-e_j,k} + u_j f_{\alpha-2e_d,k} + (\alpha_j + 1) f_{\alpha-2e_d+e_j,k}) \\ & \left. - (m+k) \frac{\partial(R T_{\text{int}})}{\partial x_j} (R T_{\text{tr}} f_{\alpha-e_j,k-1} + u_j f_{\alpha,k-1} + (\alpha_j + 1) f_{\alpha+e_j,k-1}) \right] \\ & = \text{Pr} \cdot \frac{p}{\mu} (G_{\alpha,k} - f_{\alpha,k}), \end{aligned} \quad (3.10)$$

where $f_{\beta,l}$ is taken as zero when l or any of the components of β is negative, and m is defined in (3.2).

Now we focus on the relation between $G_{\alpha,k}$ and $f_{\alpha,k}$. The expression of G (2.2)—(2.10) and the equalities under normal representation (3.7) and (3.8) show that $G_{\alpha,k}$ are functions of ρ , T_{tr} , T_{int} and $f_{e_i+e_j,0}$ with $i, j = 1, 2, 3$. Thus the system (3.10) is closed for $\alpha \in \mathbb{N}^3$ and $k = 0, 1$, which means only the expressions of $G_{\alpha,0}$ and $G_{\alpha,1}$ are needed. The following results are trivial:

$$G_{0,0} = \int_{\mathbb{R}^3 \times \mathbb{R}^+} G \, d\boldsymbol{\xi} \, dI = \rho, \quad (3.11a)$$

$$G_{e_j,0} = \int_{\mathbb{R}^3 \times \mathbb{R}^+} \xi_j G \, d\boldsymbol{\xi} \, dI - G_{0,0} u_j = 0, \quad (3.11b)$$

$$\begin{aligned} G_{0,1} &= \frac{\delta}{2} RT_{\text{int}} G_{0,0} - \int_{\mathbb{R}^3 \times \mathbb{R}^+} I^{2/\delta} G \, d\boldsymbol{\xi} \, dI \\ &= \frac{\delta}{2} \rho [RT_{\text{int}} - Z^{-1} RT_{\text{eq}} - (1 - Z^{-1}) RT_{\text{int}}] \\ &= \frac{\delta}{2Z} \rho (RT_{\text{int}} - RT_{\text{eq}}), \end{aligned} \quad (3.11c)$$

where (3.11c) comes from the physical meaning of the relaxation collision number. Moreover, since $G(\boldsymbol{\xi}, I)$ has the form

$$G(\boldsymbol{\xi}, I) = G_1(\boldsymbol{\xi}) G_2(I), \quad (3.12)$$

where

$$G_1(\boldsymbol{\xi}) = \frac{\rho}{\sqrt{\det(2\pi\mathcal{T})}} \exp\left(-\frac{1}{2}(\boldsymbol{\xi} - \mathbf{u})^T \mathcal{T}(\boldsymbol{\xi} - \mathbf{u})\right), \quad G_2(I) = \frac{\Lambda_\delta}{(RT_{\text{rel}})^{\delta/2}} \exp\left(-\frac{I^{2/\delta}}{RT_{\text{rel}}}\right), \quad (3.13)$$

and the basis functions $\psi_{\alpha,k,T_{\text{tr}},T_{\text{int}}}$ have the same structure (see (B.1))

$$\psi_{\alpha,k,T_{\text{tr}},T_{\text{int}}}(\mathbf{v}, J) = \psi_{1,\alpha,T_{\text{tr}}}(\mathbf{v}) \psi_{2,k,T_{\text{int}}}(J), \quad (3.14)$$

we can conclude

$$G_{\alpha,1} = C G_{\alpha,0}, \quad (3.15)$$

where C is independent of α . From (3.11a) and (3.11c), we find

$$C = \frac{\delta}{2Z} (RT_{\text{int}} - RT_{\text{eq}}). \quad (3.16)$$

Until now, what remains is to work out the expressions of $G_{\alpha,0}$ for $|\alpha| \geq 2$. This needs some involved calculation with details in Appendix C. The final result is in a recursive form as

$$G_{\alpha,0} = \frac{1}{\alpha_i} \sum_{j=1}^3 [(1 - \text{Pr}^{-1})(\Theta_{ij}/\rho - RT_{\text{tr}}\delta_{ij}) + Z^{-1}(RT_{\text{eq}} - RT_{\text{tr}})\delta_{ij}] G_{\alpha-e_i-e_j,0}, \quad (3.17)$$

where $i \in \{1, 2, 3\}$ such that $\alpha_i > 0$, and $G_{\alpha-e_i-e_j,0}$ is taken as zero when $\alpha_j - \delta_{ij} - 1 < 0$. With (3.11b), one can easily observe that $G_{\alpha,0} = 0$ when $|\alpha|$ is odd.

As the end of this subsection, we give the equations for the velocity \mathbf{u} and the translational and internal temperatures T_{tr} , T_{int} . The equation for u_d can be obtained by substituting α with e_d in (3.10), and the result is

$$\rho \frac{\partial u_d}{\partial t} + \sum_{j=1}^3 \left(\rho u_j \frac{\partial u_d}{\partial x_j} + \frac{\partial \Theta_{jd}}{\partial x_j} \right) = 0, \quad j = 1, 2, 3. \quad (3.18)$$

The equation for T_{tr} can be obtained by substituting α with $2e_1$, $2e_2$, $2e_3$, and then summing up all the three equations. The result is

$$\frac{\partial T_{\text{tr}}}{\partial t} + \sum_{j=1}^3 u_j \frac{\partial T_{\text{tr}}}{\partial x_j} + \frac{2}{3\rho R} \sum_{j=1}^3 \left(\frac{\partial Q_j}{\partial x_j} + \sum_{d=1}^3 \Theta_{jd} \frac{\partial u_d}{\partial x_j} \right) = \frac{\text{Pr}}{Z} \cdot \frac{p}{\mu} (T_{\text{eq}} - T_{\text{tr}}), \quad (3.19)$$

where

$$Q_j = 2f_{3e_j,0} + \sum_{d=1}^3 f_{e_j+2e_d,0}, \quad j = 1, 2, 3. \quad (3.20)$$

Similarly, if we set $\alpha = 0$ and $k = 1$, then we have

$$\frac{\partial T_{\text{int}}}{\partial t} + \sum_{j=1}^3 u_j \frac{\partial T_{\text{int}}}{\partial x_j} - \frac{2}{\delta\rho R} \sum_{j=1}^3 \frac{\partial f_{e_j,1}}{\partial x_j} = \frac{\text{Pr}}{Z} \cdot \frac{p}{\mu} (T_{\text{eq}} - T_{\text{int}}). \quad (3.21)$$

3.3 Truncation and closure with regularization

Since the moment system (3.10) contains an infinite number of equations and cannot be used for computation, we need to choose a finite set from them as the governing equations of our method. However, due to the existence of the last term in the second line of (3.10), the resulting moment system will be unclosed, which leads to the ‘‘closure problem’’ for the moment method.

We first consider the truncation of the spectral expansion. In general, we can choose two non-negative integers $M_0 \geq 2$ and $M_1 \geq 0$, and use the moment set $\{f_{\alpha,0}\}_{|\alpha| \leq M_0} \cup \{f_{\alpha,1}\}_{|\alpha| \leq M_1}$ as the finite subset. Such choice well retains the Galilean invariance since $\{f_{\alpha,0}\}$ and $\{f_{\alpha,1}\}$ only couple with each other in the collision term. We will postpone the discussion of the relation between M_0 and M_1 . Below we use \mathcal{I} to denote the index set such that the set $\{f_{\alpha,k}\}_{(\alpha,k) \in \mathcal{I}}$ contains all the moments appearing in the final moment equations.

Now we are going to make the system closed. The simplest way is to set $f_{\alpha+e_j,k} = 0$ in (3.10) if $(\alpha + e_j, k) \notin \mathcal{I}$, which leads to the Grad-type moment equations for polyatomic gases. Mallinger’s work [14] has generalize the Grad 13-moment equations to the polyatomic case. Here, we follow [17, 19, 9] and use the Maxwellian iteration together with the order of magnitude method to give a more reasonable closure. The procedure of Maxwellian iteration is constructed by rearranging (3.10) and adding superscripts repre-

senting the iteration steps:

$$\begin{aligned}
f_{\alpha,k}^{(n+1)} = & A_{\alpha,k}^{(n)} - B(\varepsilon) \left\{ \frac{\partial f_{\alpha,k}^{(n)}}{\partial t} + \sum_{d=1}^3 \frac{\partial u_d}{\partial t} f_{\alpha-e_d,k}^{(n)} \right. \\
& + \frac{1}{2} \frac{\partial(RT_{\text{tr}}^{(n+1)})}{\partial t} \sum_{d=1}^3 f_{\alpha-2e_d,k}^{(n)} - (m+k) \frac{\partial(RT_{\text{int}}^{(n+1)})}{\partial t} f_{\alpha,k-1}^{(n)} \\
& + \sum_{j=1}^3 \left[\left(RT_{\text{tr}}^{(n+1)} \frac{\partial f_{\alpha-e_j,k}^{(n)}}{\partial x_j} + u_j \frac{\partial f_{\alpha,k}^{(n)}}{\partial x_j} + (\alpha_j + 1) \frac{\partial f_{\alpha+e_j,k}^{(n)}}{\partial x_j} \right) \right. \\
& + \sum_{d=1}^3 \frac{\partial u_d}{\partial x_j} \left(RT_{\text{tr}}^{(n+1)} f_{\alpha-e_d-e_j,k}^{(n)} + u_j f_{\alpha-e_d,k}^{(n)} + (\alpha_j + 1) f_{\alpha-e_d+e_j,k}^{(n)} \right) \\
& + \frac{1}{2} \frac{\partial(RT_{\text{tr}}^{(n+1)})}{\partial x_j} \sum_{d=1}^3 \left(RT_{\text{tr}}^{(n+1)} f_{\alpha-2e_d-e_j,k}^{(n)} + u_j f_{\alpha-2e_d,k}^{(n)} + (\alpha_j + 1) f_{\alpha-2e_d+e_j,k}^{(n)} \right) \\
& \left. \left. - (m+k) \frac{\partial(RT_{\text{int}}^{(n+1)})}{\partial x_j} \left(RT_{\text{tr}}^{(n+1)} f_{\alpha-e_j,k-1}^{(n)} + u_j f_{\alpha,k-1}^{(n)} + (\alpha_j + 1) f_{\alpha+e_j,k-1}^{(n)} \right) \right] \right\}, \quad (3.22)
\end{aligned}$$

where $\varepsilon = \mu/(\text{Pr} \cdot p)$ is considered as a small parameter and (α, k) satisfies

$$(\alpha, k) \in \mathcal{S} := \{\mathbb{N}^3 \times \{0, 1\} : |\alpha| \geq 2 \text{ if } k = 0, |\alpha| \geq 1 \text{ if } k = 1\}. \quad (3.23)$$

In the first line of (3.22), $A_{\alpha,k}^{(n)}$ and $B(\varepsilon)$ are defined as

$$A_{\alpha,k}^{(n)} = \begin{cases} \frac{1}{2} \text{Pr} \cdot Z^{-1} \rho (RT_{\text{eq}} - RT_{\text{tr}}^{(n+1)}) \delta_{ij}, & \text{if } \alpha = e_i + e_j, k = 0, \\ G_{\alpha,k}^{(n)}, & \text{other cases.} \end{cases} \quad (3.24)$$

$$B(\varepsilon) = \begin{cases} \text{Pr} \cdot \varepsilon & \text{if } |\alpha| = 2, k = 0, \\ \varepsilon, & \text{other cases.} \end{cases} \quad (3.25)$$

The reason why the iteration scheme for $|\alpha| = 2$ is special is that $G_{\alpha,k}$ are functions of f_α , $|\alpha| = 2$. Note that $f_{0,0}(\rho)$, \mathbf{u} , $f_{e_j,0}(\equiv 0)$ and $f_{0,1}(\equiv 0)$ remain invariant during the iteration, and according to (3.19) and (3.21), T_{tr} and T_{int} evolves as follows:

$$T_{\text{tr}}^{(n+1)} = T_{\text{eq}} - \varepsilon Z \left[\frac{\partial T_{\text{tr}}^{(n)}}{\partial t} + \sum_{j=1}^3 u_j \frac{\partial T_{\text{tr}}^{(n)}}{\partial x_j} + \frac{2}{3\rho R} \sum_{j=1}^3 \left(\frac{\partial Q_j^{(n)}}{\partial x_j} + \sum_{d=1}^3 \Theta_{jd}^{(n)} \frac{\partial u_d}{\partial x_j} \right) \right], \quad (3.26)$$

$$T_{\text{int}}^{(n+1)} = T_{\text{eq}} - \varepsilon Z \left[\frac{\partial T_{\text{int}}^{(n)}}{\partial t} + \sum_{j=1}^3 u_j \frac{\partial T_{\text{int}}^{(n)}}{\partial x_j} - \frac{2}{\delta \rho R} \sum_{j=1}^3 \frac{\partial f_{e_j,1}^{(n)}}{\partial x_j} \right], \quad (3.27)$$

where T_{eq} also remains invariant during the iteration. The iteration starts with

$$T_{\text{tr}}^{(0)} = T_{\text{int}}^{(0)} = T_{\text{eq}}, \quad f_{0,0}^{(0)} = \rho, \quad f_{\alpha,k}^{(0)} = 0 \text{ for } (\alpha, k) \neq (0, 0). \quad (3.28)$$

In order to simplify the notation, we define the following vectors:

$$\mathbf{F}_{m,k}^{(n)} = (f_{\alpha,k}^{(n)})_{|\alpha|=m}, \quad \mathbf{F}_{[m_1,m_2],k}^{(n)} = (\mathbf{F}_{m_1,k}^{(n)}, \dots, \mathbf{F}_{m_2,k}^{(n)}), \quad m_1 < m_2. \quad (3.29)$$

and rewrite (3.22) and (3.26) as

$$f_{\alpha,k}^{(n+1)} = A_{\alpha,k}^{(n)} - \varepsilon \mathcal{L}_{\alpha,k}^{(n+1)} \cdot \mathbf{F}_{[|\alpha|-3, |\alpha|+1],k}^{(n)} + \varepsilon \mathbf{L}_{\alpha,k}^{(n+1)} \cdot \mathbf{F}_{[|\alpha|-1, |\alpha|+1],k-1}^{(n)}, \quad (3.30)$$

$$T_{\text{tr}}^{(n+1)} = T_{\text{eq}} - \varepsilon \mathcal{L}(T_{\text{tr}}^{(n)}, \mathbf{F}_{[2,3],0}^{(n)}), \quad (3.31)$$

$$T_{\text{int}}^{(n+1)} = T_{\text{eq}} - \varepsilon \mathcal{L}(T_{\text{int}}^{(n)}, \mathbf{F}_{1,1}^{(n)}), \quad (3.32)$$

where $\mathcal{L}(\cdot, \cdot)$ is a linear operator, and $\mathbf{L}_{\alpha,k}^{(n)}$ is a vector of linear operators. Each of $\mathbf{L}^{(n)}$'s components has the following form:

$$\sum_{j=1}^3 \sum_{s_1+s_2+s_3+s_4 \leq 1} \sum_{r=0}^2 C_{j,r,s} \frac{\partial^{s_1+s_2} (RT_{\text{tr}}^{(n)})^r}{\partial t^{s_1} \partial x_j^{s_2}} \frac{\partial^{s_3+s_4}}{\partial t^{s_3} \partial x_j^{s_4}}, \quad \mathbf{s} \in \{0, 1\}^4, \quad (3.33)$$

where $C_{j,r,s} = C_{j,r,s}(\rho, \mathbf{u}, \partial/\partial t, \nabla_{\mathbf{x}})$, which can be considered as a “constant” during the iteration. $\mathbf{L}_{\alpha,k}^{(n)}$ is a vector, whose components can be expressed as

$$\sum_{j=1}^3 \sum_{s_1+s_2=1, s_3+s_4 \leq 1} C_{j,s} \frac{\partial^{s_1+s_2} (RT_{\text{int}}^{(n)})}{\partial x_j^{s_1} \partial t^{s_2}} (RT_{\text{tr}}^{(n)})^{s_3} u_j^{s_4}, \quad \mathbf{s} \in \{0, 1\}^4, \quad (3.34)$$

where $C_{j,s}$ are also constants. Now we are ready to carry out the Maxwellian iteration.

The first step of iteration In the first step, the formulae for the translational and internal temperatures can be written as

$$T_{\text{tr}}^{(1)} = T_{\text{eq}} + \varepsilon S^{(0)}, \quad T_{\text{int}}^{(1)} = T_{\text{eq}} + \varepsilon U^{(0)}, \quad (3.35)$$

where $S^{(0)} \sim O(1)$ and $U^{(0)} \sim O(1)$. It is easy to find

$$G_{\alpha,k}^{(0)} = f_{\alpha,k}^{(0)}, \quad \forall \alpha \in \mathbb{N}^3, \quad k = 0, 1. \quad (3.36)$$

Thus

$$A_{\alpha,k}^{(0)} = \begin{cases} -\frac{1}{2} \varepsilon \text{Pr} \cdot Z^{-1} \rho R S^{(0)}, & \text{if } \alpha = 2e_i, k = 0, \\ 0, & \text{other cases.} \end{cases} \quad (3.37)$$

Now, it can be easily deduced from (3.30) that $f_{\alpha,k}^{(1)}$ is nonzero if and only if $0 \in [|\alpha| - 3, |\alpha| + 1]$, $k = 0$ or $0 \in [|\alpha| - 1, |\alpha| + 1]$, $k = 1$. Precisely, we have

$$f_{\alpha,k}^{(1)} \sim \begin{cases} O(\varepsilon), & (\alpha, k) \in \mathcal{S} \text{ and } |\alpha| \leq 3, k = 0, \\ O(\varepsilon), & (\alpha, k) \in \mathcal{S} \text{ and } |\alpha| = 1, k = 1, \\ 0, & \text{other cases for } (\alpha, k) \in \mathcal{S}, \end{cases} \quad (3.38)$$

and

$$\mathbf{F}_{[2,3],0}^{(1)} = \mathbf{F}_{[2,3],0}^{(0)} + \varepsilon \mathbf{H}_{[2,3],0}^{(0)}, \quad \mathbf{F}_{1,1}^{(1)} = \mathbf{F}_{1,1}^{(0)} + \varepsilon \mathbf{H}_{1,1}^{(0)}, \quad (3.39)$$

where $\mathbf{H}_{[2,3],k}^{(0)}$ and $\mathbf{H}_{1,1}^{(0)}$ has an order of magnitude $O(1)$. The meaning of the subscripts of \mathbf{H} is the same as \mathbf{F} .

Now let us consider $G_{\alpha,k}^{(1)}$. $G_{0,0}$, $G_{0,1}$ and $G_{\alpha,k}$ with odd $|\alpha|$ keep invariant during the iteration. For $G_{\alpha,0}$ with $|\alpha| \geq 2$, (3.17) gives

$$G_{\alpha,0}^{(n)} = \sum_{j=1}^3 L_{\alpha,j} \left(T_{\text{tr}}^{(n)} - T_{\text{eq}}, \mathbf{F}_{2,0}^{(n)} \right) G_{\alpha-e_i-e_j,0}^{(n)}, \quad (3.40)$$

where $L_{\alpha,j}(\cdot, \cdot)$ is a linear function independent of ε . Using (3.38), (3.35) and $G_{0,0} = \rho \sim O(1)$, we can easily get

$$G_{\alpha,0}^{(1)} \sim O(\varepsilon^{|\alpha|/2}), \quad |\alpha| \text{ is even.} \quad (3.41)$$

Using (3.16), we have

$$G_{\alpha,1}^{(1)} = \frac{\delta R}{2Z} \varepsilon U^{(0)} G_{\alpha,0}^{(1)} \sim O(\varepsilon^{|\alpha|/2+1}), \quad |\alpha| \text{ is even.} \quad (3.42)$$

The general progress In general case, we have

$$f_{\alpha,k}^{(n+1)} \sim \begin{cases} O(\varepsilon^{\lceil |\alpha|/3 \rceil}), & (\alpha, k) \in \mathcal{S} \text{ and } |\alpha| \leq 3(n+1), k=0, \\ o(\varepsilon^{\lceil |\alpha|/3 \rceil}), & (\alpha, k) \in \mathcal{S} \text{ and } |\alpha| > 3(n+1), k=0, \\ O(\varepsilon^{\lceil (|\alpha|+2)/3 \rceil}), & (\alpha, k) \in \mathcal{S} \text{ and } |\alpha| \leq 3n+1, k=1, \\ o(\varepsilon^{\lceil (|\alpha|+2)/3 \rceil}), & (\alpha, k) \in \mathcal{S} \text{ and } |\alpha| > 3n+1, k=1, \end{cases} \quad (3.43)$$

and

$$\mathbf{F}_{[2,3(n+1)],0}^{(n+1)} = \mathbf{F}_{[2,3(n+1)],0}^{(n)} + \varepsilon^{n+1} \mathbf{H}_{[2,3(n+1)],0}^{(n)}, \quad (3.44)$$

$$\mathbf{F}_{[1,3n+1],1}^{(n+1)} = \mathbf{F}_{[1,3n+1],1}^{(n)} + \varepsilon^{n+1} \mathbf{H}_{[1,3n+1],1}^{(n)}, \quad (3.45)$$

$$T_{\text{tr}}^{(n+1)} = T_{\text{tr}}^{(n)} + \varepsilon^{n+1} S^{(n)}, \quad (3.46)$$

$$T_{\text{int}}^{(n+1)} = T_{\text{int}}^{(n)} + \varepsilon^{n+1} U^{(n)}, \quad (3.47)$$

where $\mathbf{H}_{[m_1,m_2],k}^{(n)} \sim O(1)$, $S^{(n)} \sim O(1)$ and $U^{(n)} \sim O(1)$. (3.43)—(3.47) can be validated by induction. Through the derivation in the last paragraph, we have known that (3.43)—(3.47) hold for $n=0$. Now we suppose (3.43)—(3.47) hold for $n-1$. Then (3.40) gives

$$G_{\alpha,0}^{(n)} = \sum_{j=1}^3 \left[L_{\alpha,j} \left(T_{\text{tr}}^{(n-1)} - T_{\text{eq}}, \mathbf{F}_{2,0}^{(n-1)} \right) + \varepsilon^n L_{\alpha,j} \left(S^{(n-1)}, \mathbf{H}_{2,0}^{(n-1)} \right) \right] G_{\alpha-e_i-e_j,0}^{(n-1)}. \quad (3.48)$$

Now using $G_{0,0}^{(n)} = G_{0,0}^{(n-1)} = \rho$ and (3.40) with n replaced by $n-1$, simple induction gives

$$G_{\alpha,0}^{(n)} - G_{\alpha,0}^{(n-1)} \sim O(\varepsilon^{n+|\alpha|/2-1}), \quad |\alpha| \geq 2 \text{ and } |\alpha| \text{ is even.} \quad (3.49)$$

For $G_{\alpha,1}^{(n)}$, we have

$$\begin{aligned} G_{\alpha,1}^{(n)} - G_{\alpha,1}^{(n-1)} &= C^{(n)} G_{\alpha,0}^{(n)} - C^{(n-1)} G_{\alpha,0}^{(n-1)} \\ &= \left[C^{(n-1)} + \frac{\delta R}{2Z} \varepsilon^n U^{(n-1)} \right] G_{\alpha,0}^{(n)} - C^{(n-1)} G_{\alpha,0}^{(n-1)} \\ &= C^{(n-1)} (G_{\alpha,0}^{(n)} - G_{\alpha,0}^{(n-1)}) + \frac{\delta R}{2Z} \varepsilon^n U^{(n-1)} G_{\alpha,0}^{(n)} \\ &\sim O(\varepsilon) \cdot O(\varepsilon^{n+|\alpha|/2-1}) + \varepsilon^n \cdot O(1) \cdot O(\varepsilon^{|\alpha|/2}) \\ &\sim O(\varepsilon^{n+|\alpha|/2}), \quad |\alpha| \geq 2 \text{ and } |\alpha| \text{ is even.} \end{aligned} \quad (3.50)$$

Similarly, by (3.31), we have

$$\begin{aligned} T_{\text{tr}}^{(n+1)} &= T_{\text{eq}} - \varepsilon \left[\mathcal{L} \left(T_{\text{tr}}^{(n-1)}, \mathbf{F}_{[2,3],0}^{(n-1)} \right) + \varepsilon^n \mathcal{L} \left(S^{(n-1)}, \mathbf{H}_{[2,3],0}^{(n-1)} \right) \right] \\ &= T_{\text{tr}}^{(n)} - \varepsilon^{n+1} \mathcal{L} \left(S^{(n-1)}, \mathbf{H}_{[2,3],0}^{(n-1)} \right). \end{aligned} \quad (3.51)$$

Defining $S^{(n)} = -\mathcal{L} \left(S^{(n-1)}, \mathbf{H}_{[2,3],0}^{(n-1)} \right)$ gives (3.46). The validation of (3.47) is almost the same. (3.49), (3.50) and (3.51) imply that $A_{\alpha,k}^{(n)} - A_{\alpha,k}^{(n-1)}$ is never greater than $O(\varepsilon^{n+1})$.

Now it remains to consider $f_{\alpha,k}^{(n+1)}$. Similar as (3.50), the equations (3.33), (3.34) and (3.51) show

$$\mathcal{L}_{\alpha,k}^{(n+1)} - \mathcal{L}_{\alpha,k}^{(n)} \sim O(\varepsilon^{n+1}), \quad \mathcal{L}_{\alpha,k}^{(n+1)} \sim O(1), \quad (3.52)$$

$$\mathbf{L}_{\alpha,k}^{(n+1)} - \mathbf{L}_{\alpha,k}^{(n)} \sim O(\varepsilon^{n+1}), \quad \mathbf{L}_{\alpha,k}^{(n+1)} \sim O(1), \quad (3.53)$$

Using the assumptions of the induction, one has

$$\begin{aligned} f_{\alpha,0}^{(n+1)} &= A_{\alpha,0}^{(n)} - \varepsilon \mathcal{L}_{\alpha,0}^{(n+1)} \cdot \mathbf{F}_{[|\alpha|-3,|\alpha|+1],0}^{(n)} \\ &\sim \begin{cases} O(\varepsilon^{|\alpha|/2}) + \varepsilon O(1) \cdot O(\varepsilon^{\lceil(|\alpha|-3)/3\rceil}) \sim O(\varepsilon^{\lceil|\alpha|/3\rceil}), & |\alpha| \leq 3(n+1), \\ O(\varepsilon^{|\alpha|/2}) + \varepsilon O(1) \cdot o(\varepsilon^{\lceil(|\alpha|-3)/3\rceil}) \sim o(\varepsilon^{\lceil|\alpha|/3\rceil}), & |\alpha| > 3(n+1), \end{cases} \end{aligned} \quad (3.54)$$

and

$$\begin{aligned} f_{\alpha,1}^{(n+1)} &= A_{\alpha,1}^{(n)} - \varepsilon \mathcal{L}_{\alpha,1}^{(n+1)} \cdot \mathbf{F}_{[|\alpha|-3,|\alpha|+1],1}^{(n)} + \varepsilon \mathbf{L}_{\alpha,1}^{(n+1)} \cdot \mathbf{F}_{[|\alpha|-1,|\alpha|+1],0}^{(n)} \\ &\sim \begin{cases} O(\varepsilon^{|\alpha|/2+1}) + \varepsilon O(\varepsilon^{\lceil(|\alpha|-1)/3\rceil}) + \varepsilon O(\varepsilon^{\lceil(|\alpha|-1)/3\rceil}) \sim O(\varepsilon^{\lceil(|\alpha|+2)/3\rceil}), & |\alpha| \leq 3n+1, \\ O(\varepsilon^{|\alpha|/2+1}) + \varepsilon o(\varepsilon^{\lceil(|\alpha|-1)/3\rceil}) + \varepsilon o(\varepsilon^{\lceil(|\alpha|-1)/3\rceil}) \sim o(\varepsilon^{\lceil(|\alpha|+2)/3\rceil}), & |\alpha| > 3n+1. \end{cases} \end{aligned} \quad (3.55)$$

This gives (3.43). The validation of (3.44) and (3.45) needs

$$\begin{aligned} f_{\alpha,k}^{(n+1)} - f_{\alpha,k}^{(n)} &= A_{\alpha,k}^{(n)} - A_{\alpha,k}^{(n-1)} - \varepsilon (\mathcal{L}_{\alpha,k}^{(n+1)} \cdot \mathbf{F}_{[|\alpha|-3,|\alpha|+1],k}^{(n)} - \mathcal{L}_{\alpha,k}^{(n+1)} \cdot \mathbf{F}_{[|\alpha|-3,|\alpha|+1],k}^{(n-1)}) \\ &\quad + \varepsilon (\mathbf{L}_{\alpha,k}^{(n+1)} \cdot \mathbf{F}_{[|\alpha|-1,|\alpha|+1],k-1}^{(n)} - \mathbf{L}_{\alpha,k}^{(n+1)} \cdot \mathbf{F}_{[|\alpha|-1,|\alpha|+1],k-1}^{(n-1)}) \\ &= A_{\alpha,k}^{(n)} - A_{\alpha,k}^{(n-1)} - \varepsilon \mathcal{L}_{\alpha,k}^{(n+1)} \cdot (\mathbf{F}_{[|\alpha|-3,|\alpha|+1],k}^{(n)} - \mathbf{F}_{[|\alpha|-3,|\alpha|+1],k}^{(n-1)}) \\ &\quad - \varepsilon (\mathcal{L}_{\alpha,k}^{(n+1)} - \mathcal{L}_{\alpha,k}^{(n)}) \cdot \mathbf{F}_{[|\alpha|-3,|\alpha|+1],k}^{(n-1)} \\ &\quad + \varepsilon \mathbf{L}_{\alpha,k}^{(n)} \cdot (\mathbf{F}_{[|\alpha|-1,|\alpha|+1],k-1}^{(n)} - \mathbf{F}_{[|\alpha|-1,|\alpha|+1],k-1}^{(n-1)}) \\ &\quad + \varepsilon (\mathbf{L}_{\alpha,k}^{(n+1)} - \mathbf{L}_{\alpha,k}^{(n)}) \cdot \mathbf{F}_{[|\alpha|-1,|\alpha|+1],k-1}^{(n-1)}, \end{aligned} \quad (3.56)$$

and then (3.49), (3.50), (3.52) and (3.53) show that

$$f_{\alpha,k}^{(n+1)} - f_{\alpha,k}^{(n)} \sim O(\varepsilon^{n+1}). \quad (3.57)$$

The equations (3.43)–(3.45) tell us that $f_{\alpha,k}^{(n)}$ is never greater than $O(\varepsilon^{\lceil(|\alpha|+2k)/3\rceil})$ for arbitrary n , and the leading order of $f_{\alpha,k}$ appears at the $\lceil(|\alpha|+2k)/3\rceil$ -th iteration step, and never changes later. Based on these results, we can remove some high order terms in the moment equations (3.10), and the remaining part is the formula for the regularization

term. Precisely, we have

$$\begin{aligned}
& \sum_{d=1}^3 \frac{\partial u_d}{\partial t} f_{\alpha-e_d,k} + \frac{1}{2} \frac{\partial(RT_{\text{tr}})}{\partial t} \sum_{d=1}^3 f_{\alpha-2e_d,k} + \sum_{j=1}^3 RT_{\text{tr}} \frac{\partial f_{\alpha-e_j,k}}{\partial x_j} \\
& - (m+k) \frac{\partial(RT_{\text{int}})}{\partial t} f_{\alpha,k-1} + \sum_{j=1}^3 \sum_{d=1}^3 \frac{\partial u_d}{\partial x_j} (RT_{\text{tr}} f_{\alpha-e_d-e_j,k} + u_j f_{\alpha-e_d,k}) \\
& + \frac{1}{2} \sum_{j=1}^3 \frac{\partial(RT_{\text{tr}})}{\partial x_j} \sum_{d=1}^3 (RT_{\text{tr}} f_{\alpha-2e_d-e_j,k} + u_j f_{\alpha-2e_d,k} + (\alpha_j+1) f_{\alpha-2e_d+e_j,k}) \\
& - (m+k) \sum_{j=1}^3 \frac{\partial(RT_{\text{int}})}{\partial x_j} (RT_{\text{tr}} f_{\alpha-e_j,k-1} + u_j f_{\alpha,k-1} + (\alpha_j+1) f_{\alpha+e_j,k-1}) \\
& = \frac{1}{\varepsilon} (G_{\alpha,k} - f_{\alpha,k}) + h.o.t., \tag{3.58}
\end{aligned}$$

where *h.o.t.* stands for high order terms. The equations (3.18), (3.19) and (3.21) can be used to make (3.58) more compact. Noting that the terms containing $f_{e_i+e_j,0}$ or $f_{e_j,1}$ can be regarded as a high order term in (3.8), we can write (3.58) as

$$\begin{aligned}
f_{\alpha,k} = \varepsilon & \left[\sum_{j=1}^3 \left(\frac{1}{\rho} \frac{\partial(\rho RT_{\text{tr}})}{\partial x_j} f_{\alpha-e_j,k} - RT_{\text{tr}} \frac{\partial f_{\alpha-e_j,k}}{\partial x_j} \right) + \frac{1}{3} RT_{\text{tr}} \left(\sum_{j=1}^3 \frac{\partial u_j}{\partial x_j} \right) \sum_{d=1}^3 f_{\alpha-2e_d,k} \right. \\
& - \sum_{j=1}^3 \sum_{d=1}^3 \frac{1}{2} \frac{\partial(RT_{\text{tr}})}{\partial x_j} (RT_{\text{tr}} f_{\alpha-2e_d-e_j,k} + (\alpha_j+1) f_{\alpha-2e_d+e_j,k}) \\
& + (m+k) \sum_{j=1}^3 \frac{\partial(RT_{\text{int}})}{\partial x_j} (RT_{\text{tr}} f_{\alpha-e_j,k-1} + (\alpha_j+1) f_{\alpha+e_j,k-1}) \\
& \left. - \sum_{j=1}^3 \sum_{d=1}^3 \frac{\partial u_d}{\partial x_j} RT_{\text{tr}} f_{\alpha-e_d-e_j,k} \right] + G_{\alpha,k} + h.o.t.. \tag{3.59}
\end{aligned}$$

If $|\alpha| = 2$ and $k = 0$, the above equation becomes

$$\begin{aligned}
f_{e_i+e_j,0} = \varepsilon & \left[\frac{1}{3} \delta_{ij} \rho RT_{\text{tr}} \sum_{d=1}^3 \frac{\partial u_d}{\partial x_d} - \frac{1}{1+\delta_{ij}} \rho RT_{\text{tr}} \left(\frac{\partial u_i}{\partial x_j} + \frac{\partial u_j}{\partial x_i} \right) \right] \\
& + (1 - \text{Pr}^{-1}) f_{e_i+e_j,0} + \frac{1}{2} \delta_{ij} Z^{-1} \rho (RT_{\text{eq}} - RT_{\text{tr}}) + h.o.t.. \tag{3.60}
\end{aligned}$$

With (3.8), it is reformulated as

$$(1 + \delta_{ij}) f_{e_i+e_j,0} = -2\text{Pr} \cdot \varepsilon \rho RT_{\text{tr}} \frac{\partial u_{\langle i}}{\partial x_{j \rangle}} + \delta_{ij} \text{Pr} \cdot Z^{-1} \rho (RT_{\text{eq}} - RT_{\text{tr}}) + h.o.t., \tag{3.61}$$

which is similar as the Navier-Stokes law. Analogously, we can get the following relations

similar as the Fourier's law:

$$\begin{aligned} Q_j &= -\frac{5}{2}\varepsilon\rho RT_{\text{tr}}\frac{\partial(RT_{\text{tr}})}{\partial x_j} + h.o.t., \\ f_{e_j,1} &= \frac{\delta}{2}\varepsilon\rho RT_{\text{tr}}\frac{\partial(RT_{\text{int}})}{\partial x_j} + h.o.t.. \end{aligned} \quad (3.62)$$

(3.61) and (3.62) can be used to eliminate most partial derivatives in (3.59). Direct substitution gives the following result for $|\alpha| \geq 3$:

$$\begin{aligned} f_{\alpha,k} &= \varepsilon \sum_{j=1}^3 \left(\frac{1}{\rho} \frac{\partial(\rho RT_{\text{tr}})}{\partial x_j} f_{\alpha-e_j,k} - RT_{\text{tr}} \frac{\partial f_{\alpha-e_j,k}}{\partial x_j} \right) \\ &\quad + \frac{1}{2\text{Pr} \cdot \rho} \sum_{j=1}^3 \sum_{d=1}^3 (1 + \delta_{jd}) f_{e_j+e_d,0} f_{\alpha-e_d-e_j,k} \\ &\quad - \frac{1}{2} Z^{-1} (RT_{\text{eq}} - RT_{\text{tr}}) \sum_{j=1}^3 f_{\alpha-e_d-e_j,k} \\ &\quad + \frac{1}{5\rho RT_{\text{tr}}} \sum_{j=1}^3 \sum_{d=1}^3 Q_j [RT_{\text{tr}} f_{\alpha-2e_d-e_j,k} + (\alpha_j + 1) f_{\alpha-2e_d+e_j,k}] \\ &\quad + \frac{1}{\rho RT_{\text{tr}}} \sum_{j=1}^3 f_{e_j,1} [RT_{\text{tr}} f_{\alpha-e_j,k-1} + (\alpha_j + 1) f_{\alpha+e_j,k-1}] + h.o.t.. \end{aligned} \quad (3.63)$$

Neglecting the high order terms and applying the result for $|\alpha| = M_0 + 1$, $k = 0$ and $|\alpha| = M_1 + 1$, $k = 1$, we carry out a reasonable approximation to the moments of the corresponding orders. This completes the closure of the moment system.

There is still one question about the relation between M_0 and M_1 remaining. Since when $|\alpha| \geq 1$, $f_{\alpha,1}$ always has the same order of magnitude as $f_{\alpha+e_i+e_j,0}$, it is natural to choose $M_0 = M_1 + 2$. Thus the total number of moments is $(M_0 + 1)(M_0^2 + 2M_0 + 3)/3$.

3.4 Linearization of the regularization term

The expression (3.63) is rather complicated and is inconvenient for numerical implementation. In [8], we have used the technique of linearization to simplify the regularization term. Here, the same idea will be applied to derive a simplified regularization term.

We consider a local problem where the distribution function is around the Maxwellian and the variations of the density, velocity and temperature are small. Thus we have the local expansions with a small parameter ϵ indicating the magnitude of perturbation around the Maxwellian as

$$\begin{aligned} \rho &= \rho_0(1 + \epsilon\hat{p}), \quad \mathbf{u} = \mathbf{u}_0 + \epsilon\sqrt{RT_0}\hat{\mathbf{u}}, \quad T_{\text{eq}} = T_0(1 + \epsilon\hat{T}_{\text{eq}}), \quad T_{\text{tr}} = T_0(1 + \epsilon\hat{T}_{\text{tr}}), \\ \mathbf{x} &= L\epsilon\hat{\mathbf{x}}, \quad \mu = L\rho_0\sqrt{RT_0}\epsilon\hat{\mu}, \quad f_{\alpha,k} = \rho_0(RT_0)^{|\alpha|/2+k}\epsilon\hat{f}_{\alpha,k} \quad \text{for } (\alpha,k) \neq (0,0), \end{aligned} \quad (3.64)$$

where ρ_0 , \mathbf{u}_0 and T_0 are the reference density, velocity and temperature, respectively, the variables with hats $\hat{\cdot}$ are dimensionless variables with magnitudes $O(1)$ and L is the characteristic length. The equations (2.8) and (3.20) show that

$$p = \rho_0 RT_0(1 + \epsilon\hat{p}), \quad Q_j = \rho_0(RT_0)^{3/2}\epsilon\hat{Q}_j, \quad j = 1, 2, 3, \quad (3.65)$$

where \hat{p} and \hat{Q}_j are also $O(1)$ dimensionless variables. Now we put (3.64) and (3.65) into (3.63). Eliminating the constants on both sides, we get

$$\begin{aligned}
\hat{f}_{\alpha,k} = & \frac{\hat{\mu}}{\text{Pr}(1 + \epsilon\hat{p})} \sum_{j=1}^3 \left(\frac{\epsilon R}{1 + \epsilon\hat{p}} \frac{\partial(\hat{p} + \hat{T}_{\text{tr}} + \epsilon\hat{p}\hat{T}_{\text{tr}})}{\partial\hat{x}_j} \hat{f}_{\alpha-e_j,k} - R(1 + \epsilon\hat{T}_{\text{tr}}) \frac{\partial\hat{f}_{\alpha-e_j,k}}{\partial\hat{x}_j} \right) \\
& + \frac{\epsilon}{2\text{Pr}(1 + \epsilon\hat{p})} \sum_{j=1}^3 \sum_{d=1}^3 (1 + \delta_{jd}) \hat{f}_{e_j+e_d,0} \hat{f}_{\alpha-e_d-e_j,k} \\
& - \frac{1}{2} \epsilon Z^{-1} (R\hat{T}_{\text{eq}} - R\hat{T}_{\text{tr}}) \sum_{j=1}^3 \hat{f}_{\alpha-e_d-e_j,k} \\
& + \frac{\epsilon}{5(1 + \epsilon\hat{p})R(1 + \epsilon\hat{T}_{\text{tr}})} \sum_{j=1}^3 \sum_{d=1}^3 \hat{Q}_j [R(1 + \epsilon\hat{T}_{\text{tr}}) \hat{f}_{\alpha-2e_d-e_j,k} + (\alpha_j + 1) \hat{f}_{\alpha-2e_d+e_j,k}] \\
& + \frac{\epsilon}{(1 + \epsilon\hat{p})R(1 + \epsilon\hat{T}_{\text{tr}})} \sum_{j=1}^3 \hat{f}_{e_j,1} [R(1 + \epsilon\hat{T}_{\text{tr}}) \hat{f}_{\alpha-e_j,k-1} + (\alpha_j + 1) \hat{f}_{\alpha+e_j,k-1}].
\end{aligned} \tag{3.66}$$

Reserving only leading order terms on the right hand side, one has

$$\hat{f}_{\alpha,k} \approx - \frac{\hat{\mu}}{\text{Pr}(1 + \epsilon\hat{p})} \cdot R(1 + \epsilon\hat{T}_{\text{tr}}) \sum_{j=1}^3 \frac{\partial\hat{f}_{\alpha-e_j,k}}{\partial\hat{x}_j}. \tag{3.67}$$

Using (3.64) and (3.65) again, we get a simple approximation of $f_{\alpha,k}$:

$$f_{\alpha,k} \approx - \frac{\mu}{\text{Pr} \cdot p} \cdot RT_{\text{tr}} \sum_{j=1}^3 \frac{\partial f_{\alpha-e_j,k}}{\partial x_j}. \tag{3.68}$$

This approximation is to be applied to $|\alpha| = M_k + 1$ and used in our numerical method.

Remark 1. The linearization may cause the loss of accuracy in the moment method. However, since the NRxx method is applicable up to arbitrary order of moments, the loss of accuracy can be got back by increasing the highest order in the system by 1. An important advantage of the regularization term (3.68) is to smooth the profile of macroscopic variables such that the unphysical subshocks can be eliminated (see e.g. [12, 20]). We will find in the numerical experiments that the regularization term (3.68) actually acts as a diffusion.

3.5 Numerical method

The framework of the numerical scheme for the NRxx method in the polyatomic case is generally the same as that in the monatomic case. The fractional step method is utilized to treat convection term and collision term separately. For the convection term, the finite volume method with the HLL numerical flux is employed. Below we consider the one-dimensional case and suppose a uniform spatial grid with grid size Δx is used. For an arbitrary quantity ψ , the symbol ψ_i^n denotes the average value of ψ on the i -th grid at the n -th time step. Then the whole algorithm is outlined as follows:

1. Let n be zero and set $f_i^n(\xi, I)$ to be the initial value.

2. For each i , apply the technique of linear reconstruction to determine the distributions on both boundaries of the i -th grid. The results are denoted as $f_{i-1/2}^{n+}(\xi, I)$ and $f_{i+1/2}^{n-}(\xi, I)$.
3. For each reconstructed distribution function, use (3.68) for $|\alpha| = M_k + 1$ to approximate the truncated moments.
4. Use CFL condition to determine the time step Δt :

$$\Delta t \max_i \left\{ \frac{|u_i^n + C(M_0)\sqrt{(RT_{tr})_i^n}|}{\Delta x} + \frac{2(M+1)}{(\Delta x)^2} (\varepsilon RT_{tr})_i^n \right\} \leq \frac{1}{2} CFL, \quad (3.69)$$

where $C(M_0)$ is the maximal root of the Hermite polynomial $He_{M_0}(x)$, and CFL is a specified Courant number between 0 and 1.

5. Solve the convection part with the HLL scheme:

$$f_i^{n*}(\xi, I) = f_i^n(\xi, I) - \frac{\Delta t}{\Delta x} [G_{i+1/2}^n(\xi, I) - G_{i-1/2}^n(\xi, I)], \quad (3.70)$$

where

$$G_{i+1/2}^n(\xi) = \begin{cases} \xi_1 f_{i+1/2}^{n-}(\xi, I), & 0 \leq \lambda_{i+1/2}^{n-}, \\ \frac{\lambda_{i+1/2}^{n+} \xi_1 f_{i+1/2}^{n-}(\xi, I) - \lambda_{i+1/2}^{n-} \xi_1 f_{i+1/2}^{n+}(\xi, I)}{\lambda_{i+1/2}^{n+} - \lambda_{i+1/2}^{n-}} + \frac{\lambda_{i+1/2}^{n-} \lambda_{i+1/2}^{n+} [f_{i+1/2}^{n+}(\xi, I) - f_{i+1/2}^{n-}(\xi, I)]}{\lambda_{i+1/2}^{n+} - \lambda_{i+1/2}^{n-}}, & \lambda_{i+1/2}^{n-} < 0 < \lambda_{i+1/2}^{n+}, \\ \xi_1 f_{i+1/2}^{n+}(\xi, I), & 0 \geq \lambda_{i+1/2}^{n+}, \end{cases} \quad (3.71)$$

and

$$\begin{aligned} \lambda_{i+1/2}^{n-} &= \min \left\{ (u_1)_{i+1/2}^{n-} - C(M_0)\sqrt{(RT_{tr})_{i+1/2}^{n-}}, (u_1)_{i+1/2}^{n+} - C(M_0)\sqrt{(RT_{tr})_{i+1/2}^{n+}} \right\}, \\ \lambda_{i+1/2}^{n+} &= \max \left\{ (u_1)_{i+1/2}^{n-} + C(M_0)\sqrt{(RT_{tr})_{i+1/2}^{n-}}, (u_1)_{i+1/2}^{n+} + C(M_0)\sqrt{(RT_{tr})_{i+1/2}^{n+}} \right\}. \end{aligned} \quad (3.72)$$

6. Solve the collision-only equation by Δt , and the result is denoted as $f_i^{n+1}(\xi, I)$.
7. Increase n by 1 and return to Step 2.

The details of linear reconstruction and the numerical approximation of the truncated moments are almost the same as the monatomic case, and we refer the readers to [8] for our implementation. Here only Step 5 and Step 6 are expanded in the following subsections.

3.5.1 The convection step

In [7], we have mentioned that two operations are needed to accomplish the HLL scheme. One is the calculation of $\xi_j f$ for f represented by (3.5), and the other is the

linear operation on distribution functions. The former is straightforward:

$$\begin{aligned}\xi_j f(\boldsymbol{\xi}, I) &= \left(\sqrt{RT_{\text{tr}}} v_j + u_j \right) \sum_{\alpha \in \mathbb{N}^3} \sum_{k \in \mathbb{N}} f_{\alpha, k} \psi_{\alpha, k, T_{\text{tr}}, T_{\text{int}}}(\mathbf{v}, J) \\ &= \sum_{\alpha \in \mathbb{N}^3} \sum_{k \in \mathbb{N}} f_{\alpha, k} \left[RT_{\text{tr}} \psi_{\alpha+e_j, k, T_{\text{tr}}, T_{\text{int}}}(\mathbf{v}, J) + u_j \psi_{\alpha, k, T_{\text{tr}}, T_{\text{int}}}(\mathbf{v}, J) + \alpha_j \psi_{\alpha-e_j, k, T_{\text{tr}}, T_{\text{int}}}(\mathbf{v}, J) \right],\end{aligned}\quad (3.73)$$

where the recursion relation of Hermite polynomials is used, and

$$\mathbf{v} = (\boldsymbol{\xi} - \mathbf{u}) / \sqrt{RT_{\text{tr}}}, \quad J = I^{2/\delta} / (RT_{\text{int}}). \quad (3.74)$$

In order to make linear operations on distribution functions applicable, we have to solve the following problem:

For $f(\boldsymbol{\xi}, I)$ represented by (3.5), find a series of coefficients $f'_{\alpha, k}$, such that

$$f(\boldsymbol{\xi}, I) = \sum_{\alpha \in \mathbb{N}^3} \sum_{k \in \mathbb{N}} f'_{\alpha, k} \psi_{\alpha, k, T'_{\text{tr}}, T'_{\text{int}}} \left(\frac{\boldsymbol{\xi} - \mathbf{u}'}{\sqrt{RT'_{\text{tr}}}}, \frac{I^{2/\delta}}{RT'_{\text{int}}} \right)$$

for some given \mathbf{u}' , T'_{tr} and T'_{int} .

This can be tackled by two steps. First, we will find a series of coefficients $f''_{\alpha, k}$, such that

$$f(\boldsymbol{\xi}, I) = \sum_{\alpha \in \mathbb{N}^3} \sum_{k \in \mathbb{N}} f''_{\alpha, k} \psi_{\alpha, k, T_{\text{tr}}, T'_{\text{int}}} \left(\frac{\boldsymbol{\xi} - \mathbf{u}}{\sqrt{RT_{\text{tr}}}}, \frac{I^{2/\delta}}{RT'_{\text{int}}} \right). \quad (3.75)$$

Note that only $f_{\alpha, k}$'s with $k = 0, 1$ are interested, which significantly reduces the difficulty of the problem. We calculate

$$\Phi_{\alpha, k} := \int_{\mathbb{R}^3 \times \mathbb{R}^+} f(\boldsymbol{\xi}, I) \psi_{\alpha, k, T_{\text{tr}}, T_{\text{ref}}} \left(\frac{\boldsymbol{\xi} - \mathbf{u}}{\sqrt{RT_{\text{tr}}}}, \frac{I^{2/\delta}}{RT_{\text{ref}}} \right) \exp \left(\frac{|\boldsymbol{\xi} - \mathbf{u}|^2}{2RT_{\text{tr}}} + \frac{I^{2/\delta}}{RT_{\text{ref}}} \right) d\boldsymbol{\xi} dI \quad (3.76)$$

using both (3.5) and (3.75), where T_{ref} is an arbitrary positive real number. Thanks to the orthogonality of Hermite and Laguerre polynomials, the results can be obtained as

$$\Phi_{\alpha, 0} = C_0 f_{\alpha, 0} = C_0 f''_{\alpha, 0}, \quad (3.77)$$

$$\Phi_{\alpha, 1} = C_1 \left[f_{\alpha, 1} + \frac{\delta}{2} (RT_{\text{ref}} - RT_{\text{int}}) f_{\alpha, 0} \right] = C_1 \left[f''_{\alpha, 1} + \frac{\delta}{2} (RT_{\text{ref}} - RT'_{\text{int}}) f''_{\alpha, 0} \right], \quad (3.78)$$

where

$$C_0 = \frac{2}{\delta} \frac{\alpha!}{(2\pi)^{3/2}} \Gamma(m+1) (RT_{\text{tr}})^{-(|\alpha|+3)} (RT_{\text{ref}})^{-\delta/2}, \quad (3.79)$$

$$C_1 = \frac{2}{\delta} \frac{\alpha!}{(2\pi)^{3/2}} \Gamma(m+2) (RT_{\text{tr}})^{-(|\alpha|+3)} (RT_{\text{ref}})^{-(\delta/2+2)}. \quad (3.80)$$

With (3.77) and (3.78), we immediately get

$$f''_{\alpha, 0} = f_{\alpha, 0}, \quad f''_{\alpha, 1} = f_{\alpha, 1} + \frac{\delta}{2} (RT'_{\text{int}} - RT_{\text{int}}) f_{\alpha, 0}. \quad (3.81)$$

The second step is to calculate $f'_{\alpha,k}$ from $f''_{\alpha,k}$. Since the scaling factor on the I -axis RT'_{int} is not changed in such transformation, we can use the very technique introduced in [7] to obtain $f'_{\alpha,k}$ efficiently. Specifically speaking, we define

$$F(\mathbf{v}, J, \tau) = \sum_{\alpha \in \mathbb{N}^3} \sum_{k \in \mathbb{N}} F_{\alpha,k}(\tau) [(\hat{T} - 1)\tau + 1]^{|\alpha|+3} \psi_{\alpha,k,T_{\text{tr}},T'_{\text{int}}} \left([(\hat{T} - 1)\tau + 1]\mathbf{v} + \tau\mathbf{w}, J \right), \quad (3.82)$$

where

$$\hat{T} = \sqrt{\frac{T_{\text{tr}}}{T'_{\text{tr}}}}, \quad \mathbf{w} = \frac{\mathbf{u} - \mathbf{u}'}{\sqrt{RT'_{\text{tr}}}}, \quad \tau \in [0, 1]. \quad (3.83)$$

If we require

$$\frac{\partial F}{\partial \tau} \equiv 0, \quad \forall \tau \in [0, 1], \quad \text{and} \quad F_{\alpha,k}(0) = f''_{\alpha,k}, \quad \forall (\alpha, k) \in \mathbb{N}^3 \times \mathbb{N}, \quad (3.84)$$

then it is easy to find $F_{\alpha,k}(1) = f'_{\alpha,k}$, $\forall (\alpha, k) \in \mathbb{N}^3 \times \mathbb{N}$. The next job is to write $\frac{\partial F}{\partial \tau}$ in the form of (3.5), and then require each coefficient to be zero. Thus an ordinary differential system is obtained. The calculation of $\frac{\partial F}{\partial \tau}$ is almost a repetition of that presented in [7], which is omitted here. The resulting ordinary differential equations are

$$\begin{cases} \frac{dF_{\alpha,k}}{d\tau} = [1 - \tau S(\tau)]^2 \sum_{d=1}^3 \left[S(\tau) RT_{\text{tr}} F_{\alpha-2e_d,k} + (u_d - u'_d) \hat{T} F_{\alpha-e_d,k} \right], \\ F_{\alpha,k}(0) = f''_{\alpha,k}, \end{cases} \quad (3.85)$$

where

$$S(\tau) = \frac{\hat{T} - 1}{(\hat{T} - 1)\tau + 1}. \quad (3.86)$$

In our implementation, we solve (3.85) using Runge-Kutta method until $\tau = 1$, and then $F_{\alpha,k}(1) = f'_{\alpha,k}$ can be obtained. The readers can find some properties of (3.85) in [7]. Equations (3.81) and (3.85) give a practical way to calculate $f'_{\alpha,k}$ for $k = 0, 1$.

3.5.2 The collision step

It remains to give a numerical method to solve the collision-only equation

$$\frac{\partial f}{\partial t} = \frac{1}{\varepsilon} (G - f) \quad (3.87)$$

by one time step. The corresponding moment equations can be extracted from (3.10) by removing the terms arising in the convection term. This results

$$\frac{\partial f_{\alpha,k}}{\partial t} + \sum_{d=1}^3 \frac{\partial u_d}{\partial t} f_{\alpha-e_d,k} + \frac{1}{2} \frac{\partial(RT_{\text{tr}})}{\partial t} \sum_{d=1}^3 f_{\alpha-2e_d,k} - (m+k) \frac{\partial(RT_{\text{int}})}{\partial t} f_{\alpha,k-1} = \frac{1}{\varepsilon} (G_{\alpha,k} - f_{\alpha,k}). \quad (3.88)$$

Let $(\alpha, k) = (0, 0)$ and $(\alpha, k) = (e_j, 0)$ respectively, and one has

$$\frac{\partial \rho}{\partial t} = 0, \quad \frac{\partial u_j}{\partial t} = 0. \quad (3.89)$$

Thus the second term in (3.88) vanishes. Let $(\alpha, k) = (2e_j, 0)$, $j = 1, 2, 3$ and sum the equations up, and we get

$$\frac{\partial T_{\text{tr}}}{\partial t} = \frac{1}{\varepsilon Z} (T_{\text{eq}} - T_{\text{tr}}) \quad (3.90)$$

Setting $(\alpha, k) = (0, 1)$ in (3.88), it becomes

$$\frac{\partial T_{\text{int}}}{\partial t} = \frac{1}{\varepsilon Z} (T_{\text{eq}} - T_{\text{int}}). \quad (3.91)$$

Using (2.7), it is easy to obtain

$$\frac{\partial T_{\text{eq}}}{\partial t} = 0. \quad (3.92)$$

Equations (3.89) and (3.92) agree with the fact that the density, velocity and temperature are not changed by collision. Now (3.88) can be rewritten as

$$\frac{\partial f_{\alpha,k}}{\partial t} = \frac{1}{\varepsilon} \left[G_{\alpha,k} - f_{\alpha,k} - Z^{-1} (RT_{\text{eq}} - RT_{\text{tr}}) \left(\frac{1}{2} \sum_{j=1}^3 f_{\alpha-2e_j,k} - (m+k) f_{\alpha,k-1} \right) \right]. \quad (3.93)$$

Setting $(\alpha, k) = (e_i + e_j, 0)$ in (3.17) and substituting the result into (3.93), one finds that the collision-only equation for $f_{e_i+e_j,0}$ has also a simple form:

$$\frac{\partial f_{e_i+e_j,0}}{\partial t} = -\frac{1}{\varepsilon \text{Pr}} f_{e_i+e_j,0}, \quad i, j = 1, 2, 3, \quad (3.94)$$

which agrees with the settings in [6]. Now suppose we want to solve (3.87) from t^n to t^{n+1} . For simplicity, for any quantity ψ , we use ψ^n , ψ^{n+1} and $\psi^{n+1/2}$ to denote $\psi(t^n)$, $\psi(t^{n+1})$ and $\psi(\frac{1}{2}(t^n + t^{n+1}))$, respectively. Then the following relations holds analytically for $i, j = 1, 2, 3$ and $t \in [t^n, t^{n+1}]$:

$$\begin{aligned} \rho(t) &\equiv \rho^n, & u_j(t) &\equiv u_j^n, & T_{\text{eq}}(t) &\equiv T_{\text{eq}}^n, \\ T_{\text{tr}}(t) &= T_{\text{eq}}^n + (T_{\text{tr}}^n - T_{\text{eq}}^n) \exp\left(-\frac{t-t^n}{\varepsilon Z}\right), \\ T_{\text{int}}(t) &= T_{\text{eq}}^n + (T_{\text{int}}^n - T_{\text{eq}}^n) \exp\left(-\frac{t-t^n}{\varepsilon Z}\right), \\ f_{e_i+e_j,0}(t) &= f_{e_i+e_j,0}^n \exp\left(-\frac{t-t^n}{\varepsilon \text{Pr}}\right). \end{aligned} \quad (3.95)$$

These are deduced from (3.89)—(3.92) and (3.94). Based on (3.95), $G_{\alpha,k}(t)$ can also be obtained since it can be observed from (3.11) and (3.15)—(3.17) that $G_{\alpha,k}$ are fully determined by the variables listed in (3.95). For other cases, meaning $|\alpha| > 2$ if $k = 0$ and $|\alpha| > 0$ if $k = 1$, the Crank-Nicolson scheme is employed to give a numerical approximation of (3.93):

$$\begin{aligned} \frac{f_{\alpha,k}^{n+1} - f_{\alpha,k}^n}{\Delta t} &= \frac{1}{\varepsilon} \left[G_{\alpha,k}^{n+1/2} - \frac{f_{\alpha,k}^{n+1} + f_{\alpha,k}^n}{2} - Z^{-1} \left(RT_{\text{eq}}^{n+1/2} - RT_{\text{tr}}^{n+1/2} \right) \times \right. \\ &\quad \left. \left(\frac{1}{2} \sum_{j=1}^3 \frac{f_{\alpha-2e_j,k}^{n+1} + f_{\alpha-2e_j,k}^n}{2} - (m+k) \frac{f_{\alpha,k-1}^{n+1} + f_{\alpha,k-1}^n}{2} \right) \right], \end{aligned} \quad (3.96)$$

where $\Delta t = t^{n+1} - t^n$. Note that no linear system needs to be solved when applying (3.96), since when solving $f_{\alpha,k}^{n+1}$, the terms $f_{\alpha-2e_j,k}^{n+1}$ and $f_{\alpha,k-1}^{n+1}$ have always been obtained, and then (3.96) is simply a linear equation of $f_{\alpha,k}^{n+1}$.

Remark 2. When $\text{Pr} = Z = 1$, one has $\mathcal{T} = RT_{\text{eq}}\text{Id}$ and $T_{\text{rel}} = T_{\text{eq}}$ in (2.2). Obviously, in this case, the ES-BGK model reduces to the BGK model, and the above technique for processing the collision terms is still valid.

4 Numerical examples

In this section, two one-dimensional numerical examples are presented to validate our algorithm. The spatial variable \mathbf{x} will be written in plain font as x . For both tests, the non-dimensional form of the Boltzmann equation (2.1) is used. Thus the gas constant R is chosen as 1, and the Knudsen number Kn , which is the ratio of the mean free path to the characteristic length, controls the rarefaction of the gas. Only the diatomic gas is considered below; therefore δ equals to 2.0. The CFL number is set to be 0.95 in all runs.

4.1 Shock tube test

There have been a number of studies on using the moment method to solve shock tube problems. In [22], the 13-moment case is carefully investigated and the numerical results in [5, 23] indicate that the theory for 13-moment case can also be applied to systems with almost any number of moments. And in [7, 9], the shock tube problem in the monatomic case is calculated to show the convergence of the original NRxx method and its improved version when the number of moments increases. Here the similar settings are used the test the polyatomic NRxx method. The initial conditions are

$$f(0, x, \boldsymbol{\xi}, I) = \begin{cases} \rho_l \psi_{0,0,T_l,T_l}(\boldsymbol{\xi}/\sqrt{T_l}, I/T_l), & x < 0, \\ \rho_r \psi_{0,0,T_r,T_r}(\boldsymbol{\xi}/\sqrt{T_r}, I/T_r), & x > 0, \end{cases} \quad (4.1)$$

where $\rho_l = 7$, $\rho_r = 1$, and $T_l = T_r = 1$. Recalling that $R = 1$ and $\delta = 2$, we find the fluid states on both left and right sides are in equilibrium. As an artificial test, a simple expression for the viscosity coefficient μ is chosen as

$$\mu = Kn \cdot T_{\text{eq}}. \quad (4.2)$$

Four additional parameters, including the Prandtl number Pr , the relaxation collision number Z , the Knudsen number Kn , and the maximal moment order M_0 , need to be defined for this problem. Below, different combinations of these parameters are tested in our numerical examples to show different properties of the polyatomic NRxx method. In all the experiments, the computational domain is $[-2, 2]$ and discretized using 400 uniform spatial grids. In the following subsections, all plots show the numerical results at $t = 0.3$.

4.1.1 Convergence in the number of moments

In this part, we set $\text{Pr} = 0.72$ and $Z = 5$, and test the behavior of solutions for several Knudsen numbers when M_0 increases. In order to provide a reference solution, Mieussens' conservative discrete velocity model (CDVM) [16, 10] is computed. For CDVM, we use the technique of dimension reduction to speed up the computation. That is, we define

$$\begin{aligned} g(t, x, \xi_1) &= \int_{\mathbb{R}^2 \times \mathbb{R}^+} f(t, x, \boldsymbol{\xi}, I) d\xi_2 d\xi_3 dI, \\ h_1(t, x, \xi_1) &= \frac{1}{2} \int_{\mathbb{R}^2 \times \mathbb{R}^+} (\xi_2^2 + \xi_3^2) f(t, x, \boldsymbol{\xi}, I) d\xi_2 d\xi_3 dI, \\ h_2(t, x, \xi_1) &= \int_{\mathbb{R}^2 \times \mathbb{R}^+} I f(t, x, \boldsymbol{\xi}, I) d\xi_2 d\xi_3 dI, \end{aligned} \quad (4.3)$$

and solve g , h_1 and h_2 instead of the distributions with full three-dimensional microscopic velocity. The velocity space is discretized by 400 grids. Currently, this skill is not used in the NRxx method.

First, a relatively dense case $Kn = 0.05$ is considered. The density and equilibrium temperature results for $M_0 = 3, \dots, 8$ are given in Figure 1. For $M_0 \geq 5$, the NRxx results match with the CDVM results very well. This agrees with the observation in [7, 9] that for small Knudsen numbers, a small number of moments can describe the macroscopic quantities in a high accuracy. The results for a rarefied case $Kn = 0.5$ from $M_0 = 3$ to $M_0 = 20$ are presented in Figure 2. It is obvious that in order to match the CDVM results, much greater number of moments are needed. However, we can still find the NRxx results converge as M_0 increases, and the limit is probably the solution of the Boltzmann equation.

Now we consider a severe case $Kn = 5$, and the results are given in Figure 3. Although the NRxx solutions deviate from the reference solution greater than those in Figure 2, the convergence is again very clear. From Figure 1—3, we can find the theory in [22] is also valid for the regularized moment methods. For a fixed choice of M_0 , the corresponding moment system always fails to describe the physical phenomenon when $t \rightarrow 0$ (or $Kn \rightarrow \infty$ for a fixed time t) due to the very strong non-equilibrium. As t increases, the collision term starts to show an effect of dissipation, and the solution of the moment system gradually presents its physical meaning. As is shown in [5, 23], for a greater M_0 , such progress is faster. Our numerical results correctly exhibit this behavior.

4.1.2 Comparison between BGK and ES-BGK collision terms

As is known, for monatomic gases, the BGK model fails to predict the correct Prandtl number, while Pr is considered as a parameter in the ES-BGK collision term. For polyatomic gases, besides the Prandtl number, the BGK model also gives incorrect relaxation collision number Z . Actually, the BGK model always gives $Z = 1$, which means the translational and internal temperatures tend to the equilibrium temperature more rapidly than the ES-BGK model. Thus it can be expected that the BGK model gives incorrect translational temperature, internal temperature, and heat fluxes.

As a test, we set $Pr = 0.72$, $Z = 5$, $Kn = 0.05$ and $M_0 = 5$, and both BGK and ES-BGK collision models are computed. The results are shown in Figure 4 and Figure 5. In Figure 4, it is found that the BGK model gives a pretty good prediction of the density, whereas the deviation of temperature between two models is significant. Figure 5 shows that the BGK model provides much smaller difference between the translational temperature and the internal temperature than the ES-BGK model, which indicates different relaxation collision numbers involved in the two models. The heat flux q_1 is defined as

$$q_1 = \int_{\mathbb{R}^3 \times \mathbb{R}^+} (\xi_1 - u_1) \left(\frac{1}{2} |\boldsymbol{\xi} - \mathbf{u}|^2 + I^{2/\delta} \right) f(\boldsymbol{\xi}, I) d\boldsymbol{\xi} dI. \quad (4.4)$$

The difference in the heat flux is caused by the discordance of both the Prandtl number and the relaxation collision number.

4.1.3 Comparison between the monatomic case and the polyatomic case

Let $Z = \infty$ and define

$$g(t, \mathbf{x}, \boldsymbol{\xi}) = \int_{\mathbb{R}^+} f(t, \mathbf{x}, \boldsymbol{\xi}, I) dI. \quad (4.5)$$

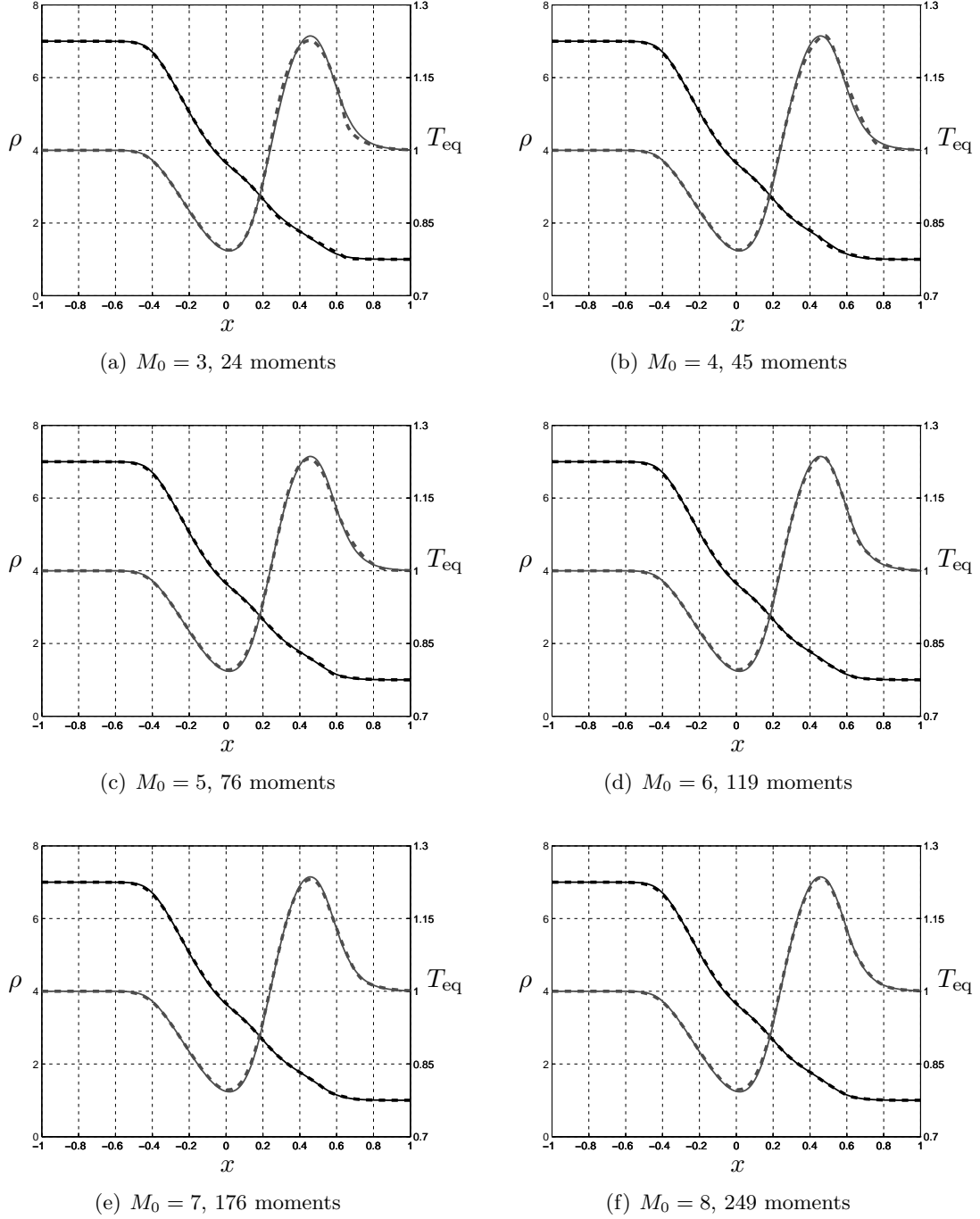
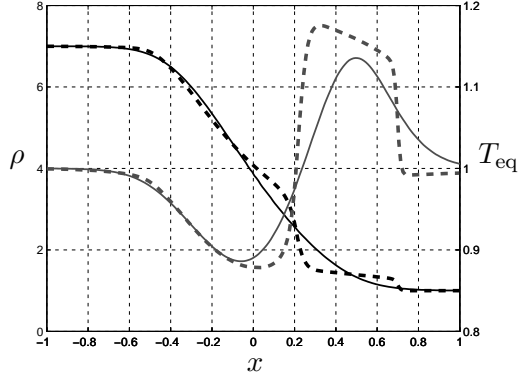
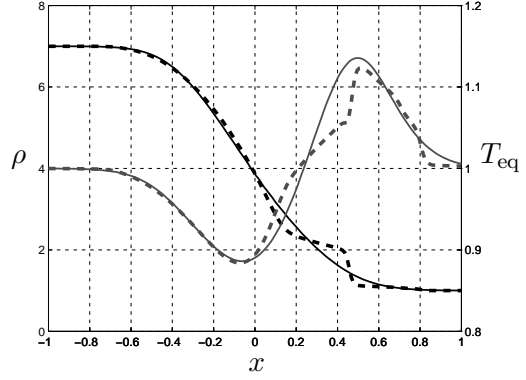


Figure 1: Numerical results for the shock tube problem with $Kn = 0.05$. The dashed lines are the NRxx results, and the solid thin lines are the CDVM results with linearization. The dashdot lines are the results of discrete velocity model. The black lines denote the density ρ and the gray lines denote the equilibrium temperature T_{eq} .

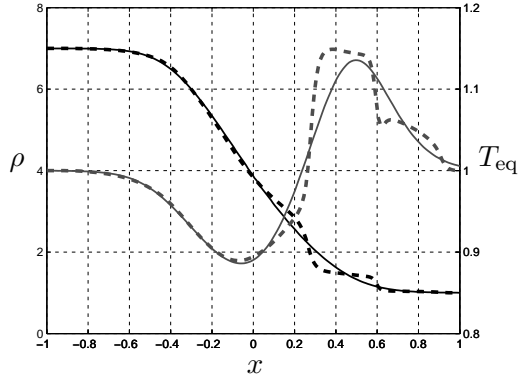
Integrating the both sides of (2.1) over \mathbb{R}^+ with respect to I , it is not difficult to find that the reduced distribution function g satisfies the monatomic Boltzmann equation with ES-BGK collision operator. Thus, it is natural to expect that when the relaxation collision



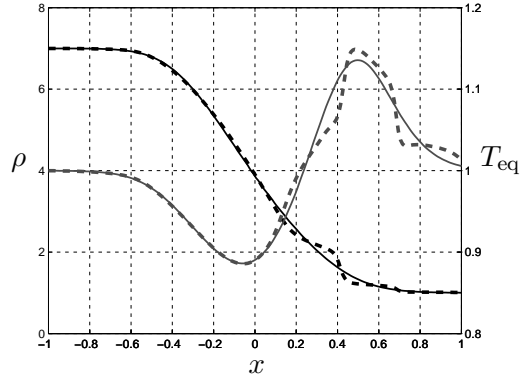
(a) $M_0 = 3$, 24 moments



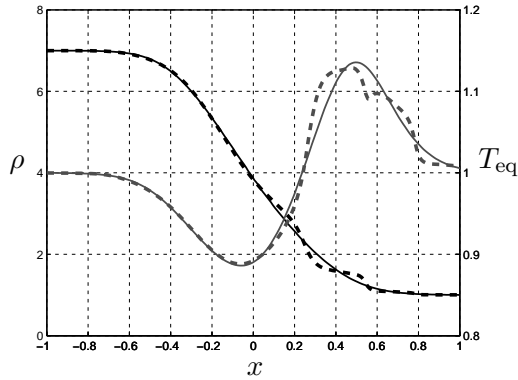
(b) $M_0 = 4$, 45 moments



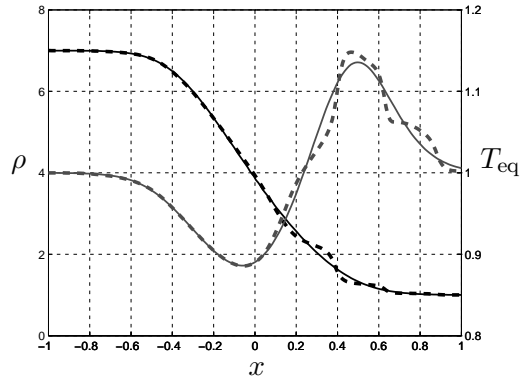
(c) $M_0 = 5$, 76 moments



(d) $M_0 = 6$, 119 moments



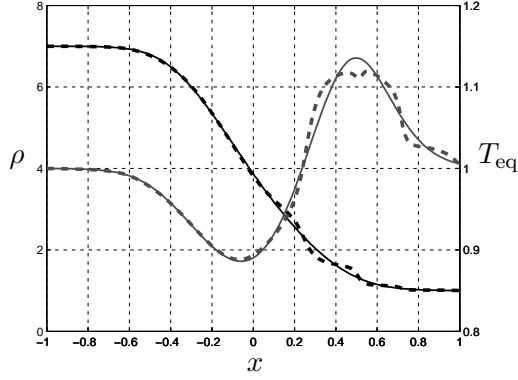
(e) $M_0 = 7$, 176 moments



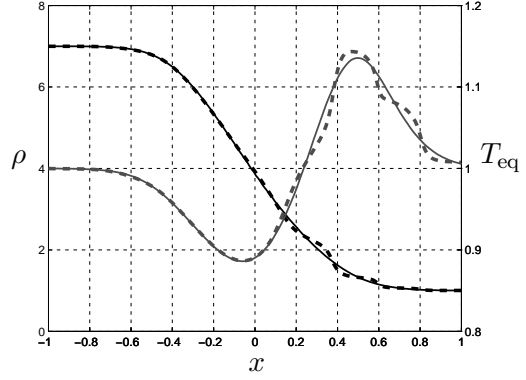
(f) $M_0 = 8$, 249 moments

Figure 2: Numerical results for the shock tube problem with $Kn = 0.5$. The dashed lines are the NRxx results, and the solid thin lines are the CDVM results with linearization. The dashdot lines are the results of discrete velocity model. The black lines denote the density ρ and the gray lines denote the equilibrium temperature T_{eq} (continued on the next page).

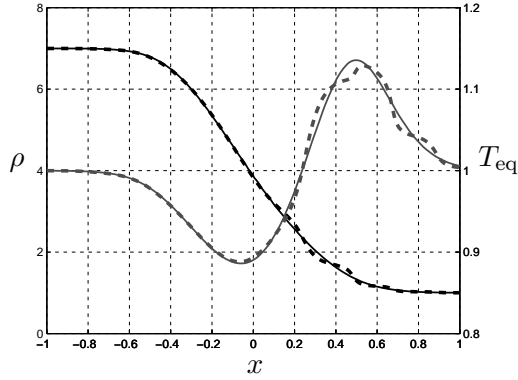
number Z gets greater, the polyatomic case will get closer to the monatomic case. The part is devoted to the numerical validation of this behavior.



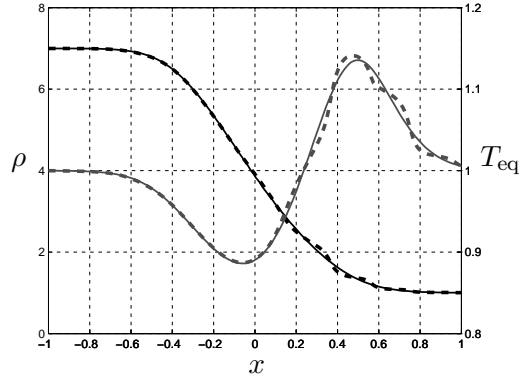
(g) $M_0 = 9$, 340 moments



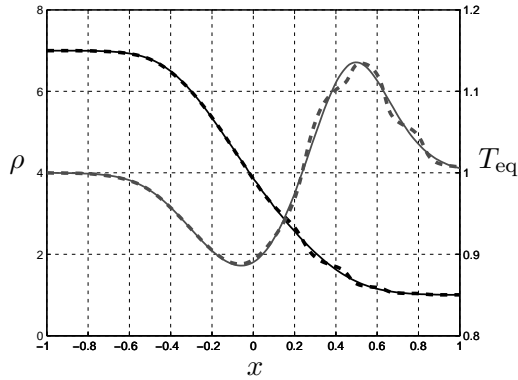
(h) $M_0 = 10$, 451 moments



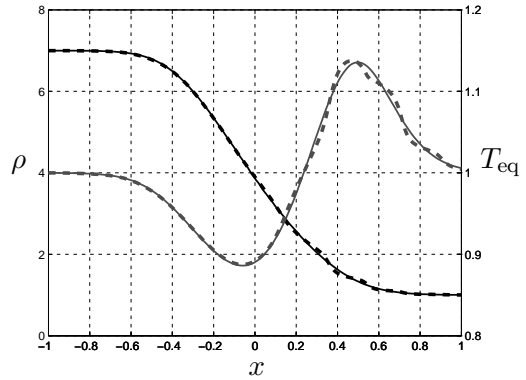
(i) $M_0 = 11$, 584 moments



(j) $M_0 = 12$, 741 moments



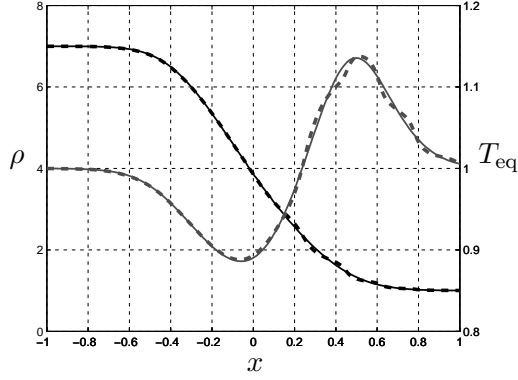
(k) $M_0 = 13$, 924 moments



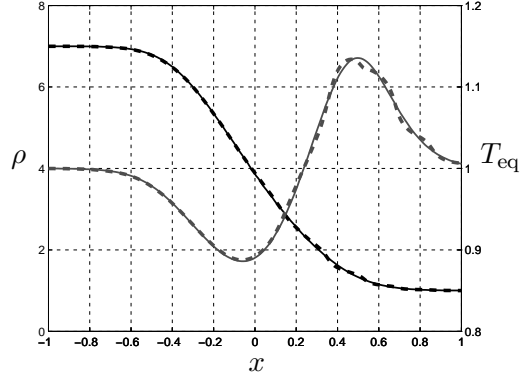
(l) $M_0 = 14$, 1135 moments

Figure 2 (continued): Numerical results for the shock tube problem with $Kn = 0.5$. The dashed lines are the NRxx results, and the solid thin lines are the CDVM results with linearization. The dashdot lines are the results of discrete velocity model. The black lines denote the density ρ and the gray lines denote the equilibrium temperature T_{eq} (continued on the next page).

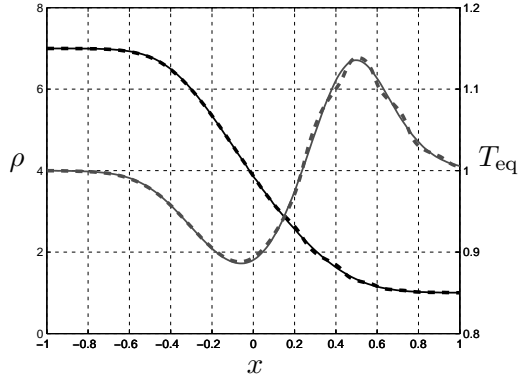
The NRxx method for monatomic gases has been introduced in [7, 9, 8], where a BGK collision model is considered. For the monatomic ES-BGK model, the collision



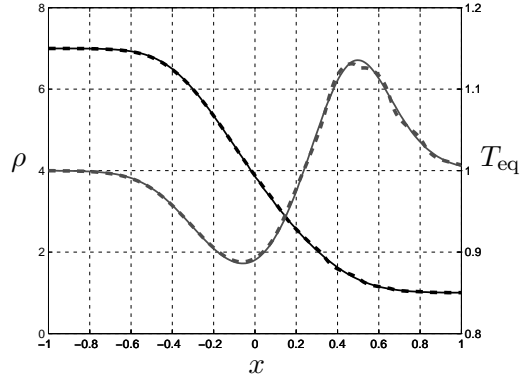
(m) $M_0 = 15$, 1376 moments



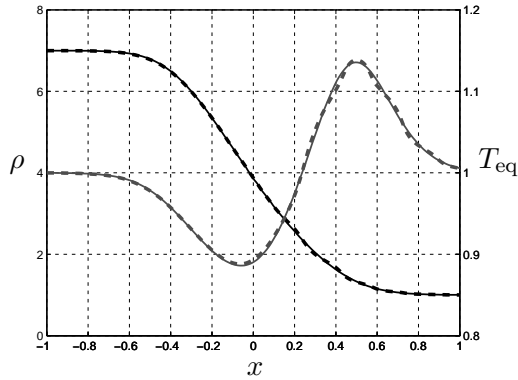
(n) $M_0 = 16$, 1649 moments



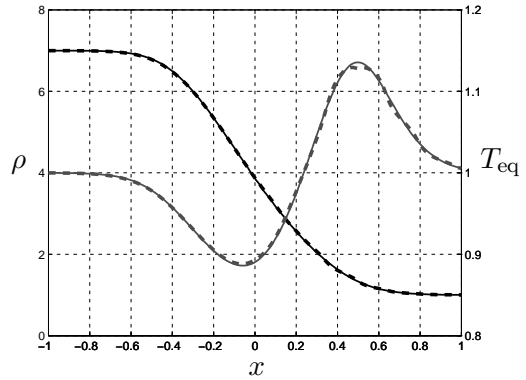
(o) $M_0 = 17$, 1956 moments



(p) $M_0 = 18$, 2299 moments



(q) $M_0 = 19$, 2680 moments



(r) $M_0 = 20$, 3101 moments

Figure 2 (continued): Numerical results for the shock tube problem with $Kn = 0.5$. The dashed lines are the NRxx results, and the solid thin lines are the CDVM results with linearization. The dashdot lines are the results of discrete velocity model. The black lines denote the density ρ and the gray lines denote the equilibrium temperature T_{eq} .

only equation can be analytically solved, and the result will be reported elsewhere. Four relaxation collision numbers $Z = 1, 10, 100, 1000$ are considered here, and other parameters are $Pr = 2/3$, $Kn = 0.01$, $M_0 = 5$. The numerical results can be found in Figure 6. It

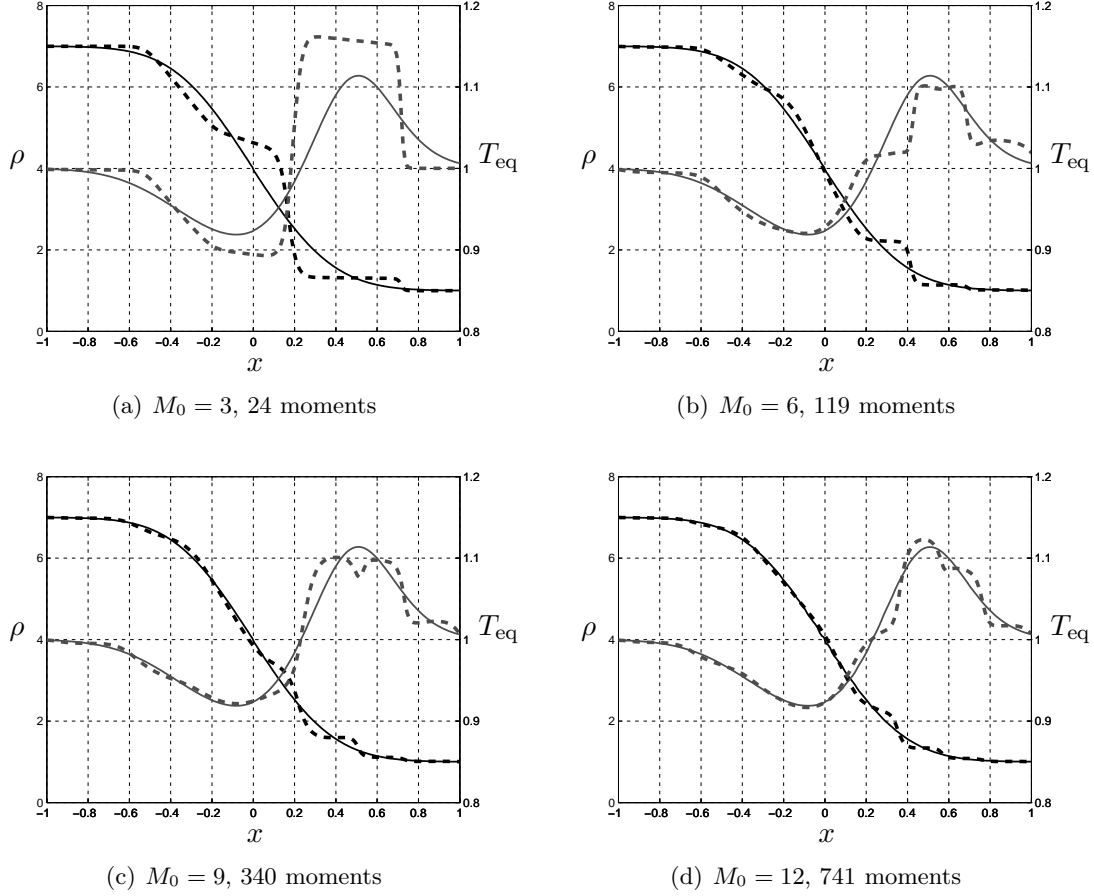


Figure 3: Numerical results for the shock tube problem with $Kn = 5.0$. The dashed lines are the NRxx results, and the solid thin lines are the CDVM results with linearization. The dashdot lines are the results of discrete velocity model. The black lines denote the density ρ and the gray lines denote the equilibrium temperature T_{eq} (continued on the next page).

clearly shows that the polyatomic result tends to the monatomic result gradually as Z increases.

4.2 Shock structure of nitrogen

In this section, we will use the polyatomic NRxx method to compute the shock structure of nitrogen, trying to reproduce the experimental results reported in [2]. In order to get a steady shock structure with Mach number Ma , we solve a Riemann problem with the following initial condition until a steady state:

$$f(0, x, \boldsymbol{\xi}, I) = \begin{cases} \rho_l \psi_{0,0,T_l,T_l}((\boldsymbol{\xi} - \mathbf{u}_l)/\sqrt{T_l}, I/T_l), & x < 0, \\ \rho_r \psi_{0,0,T_r,T_r}((\boldsymbol{\xi} - \mathbf{u}_r)/\sqrt{T_r}, I/T_r), & x > 0, \end{cases} \quad (4.6)$$

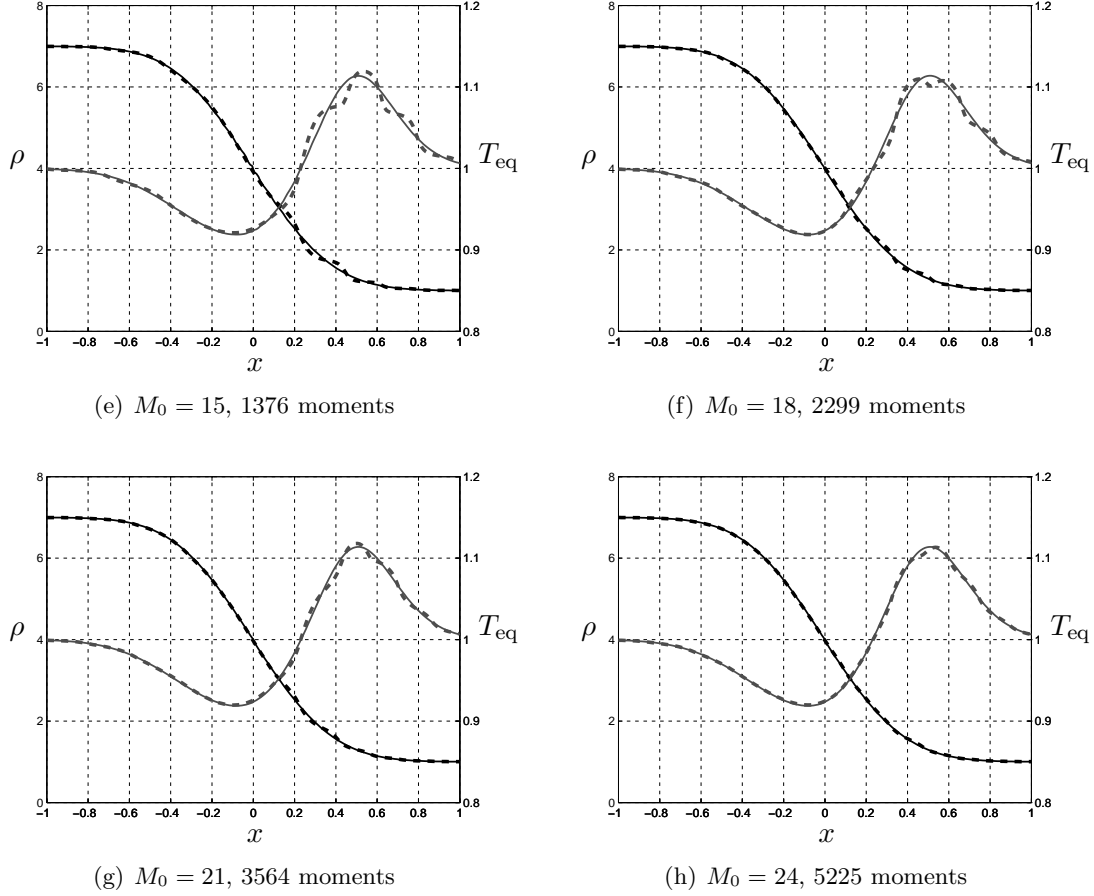


Figure 3 (continued): Numerical results for the shock tube problem with $Kn = 5.0$. The dashed lines are the NRxx results, and the solid thin lines are the CDVM results with linearization. The dashdot lines are the results of discrete velocity model. The black lines denote the density ρ and the gray lines denote the equilibrium temperature T_{eq} .

where

$$\begin{aligned} \rho_l &= 1, \quad \mathbf{u}_l = (\sqrt{\gamma}Ma, 0, 0)^T, \quad T_l = 1, \\ \rho_r &= \frac{(\gamma + 1)Ma^2}{(\gamma - 1)Ma^2 + 2}, \quad \mathbf{u}_r = \frac{\rho_l}{\rho_r} \mathbf{u}_l, \quad T_r = \frac{2\gamma Ma^2 - (\gamma - 1)}{(\gamma + 1)\rho_r}. \end{aligned} \quad (4.7)$$

Here γ is the adiabatic index. For nitrogen, γ equals to 1.4. The Prandtl number is chosen as 0.72 as in [24]. The Knudsen number is $Kn = 0.1$, and the grid size is $\Delta x = 0.005$. The computational domain is $[-1.5, 1.5]$, which is large enough to cover the whole shock structure.

It remains to give the expressions of Z and μ . They have significant influence on the thickness of the shock. For the relaxation collision number Z , both the gas-kinetic model [24] and the direct simulation Monte Carlo (DSMC) [2] show that $Z = 4$ or $Z = 5$ best fits the experimental data. However, in both [13] and [3], where the Rykov and ES-BGK models are used respectively, it is reported that a smaller Z between 2 and 3 gives better numerical results. The same conclusion is drawn by our numerical experiments. Since [13]

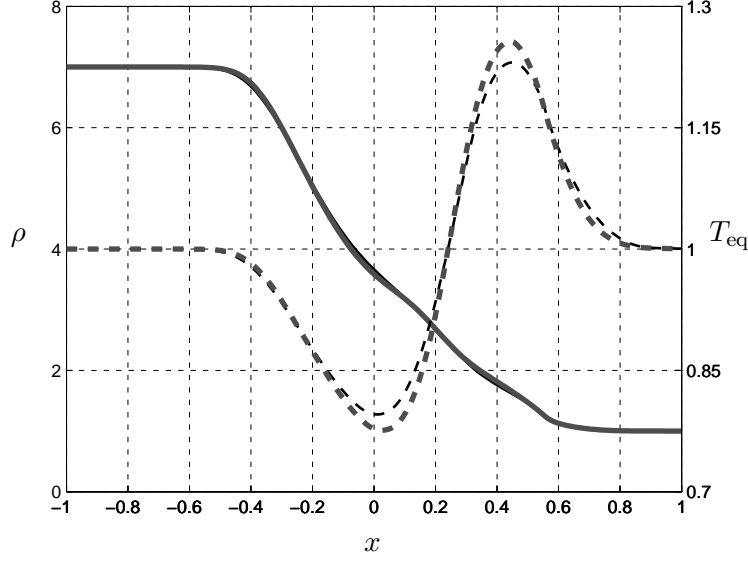


Figure 4: Comparison between BGK and ES-BGK models. The black lines are the results of the ES-BGK model, and the gray lines are the results of the BGK model. The solid lines denote the profile of density ρ , and the dashed lines denote the profile of equilibrium temperature T_{eq} .

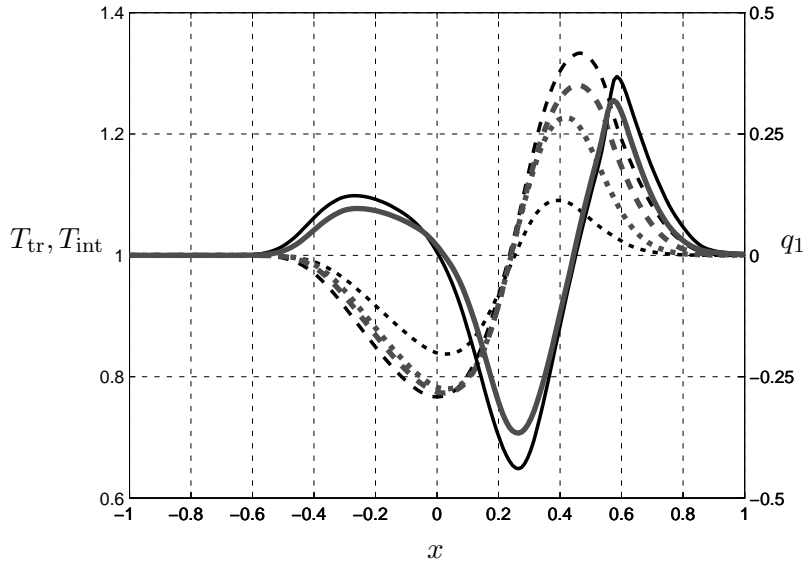
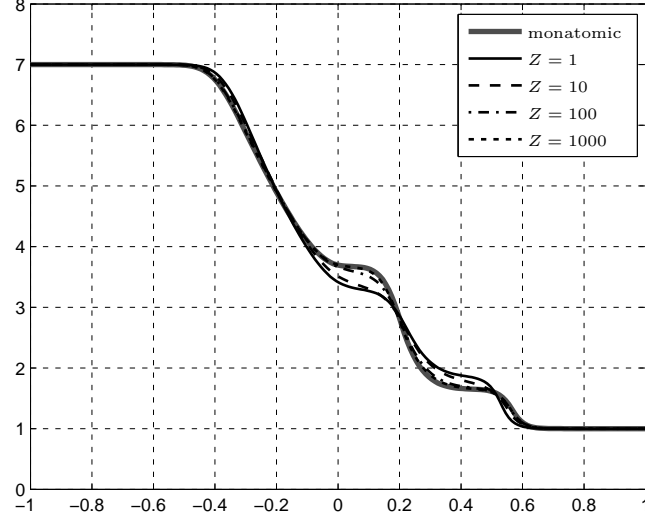


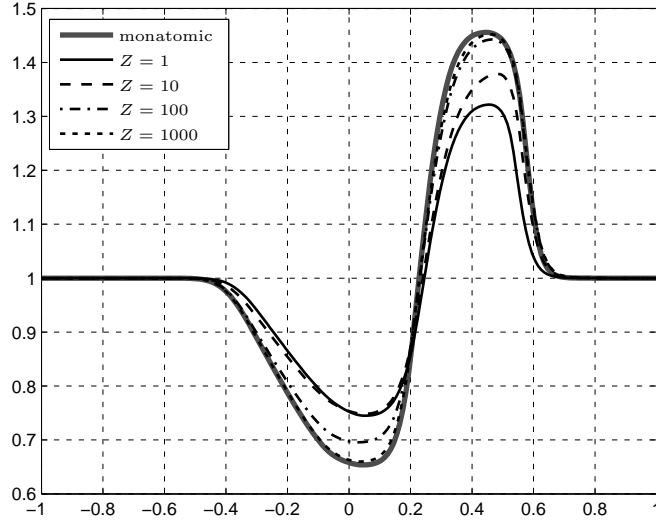
Figure 5: Comparison between BGK and ES-BGK models. The black lines are the results of the ES-BGK model, and the gray lines are the results of the BGK model. The dashed and dotted lines denote the profile of translational temperature T_{tr} and internal temperature T_{int} , respectively, and the solid lines denote the heat flux q_1 .

also considers the shock structure problem, we use the same settings here:

$$\mu = \frac{5}{8} \sqrt{\frac{\pi}{2}} Kn T_{\text{eq}}^{0.72}, \quad Z = 1.45 \left(1 + 0.75 \frac{T_{\text{int}}}{T_{\text{tr}}} \right). \quad (4.8)$$



(a) Density profile



(b) Translational temperature profile

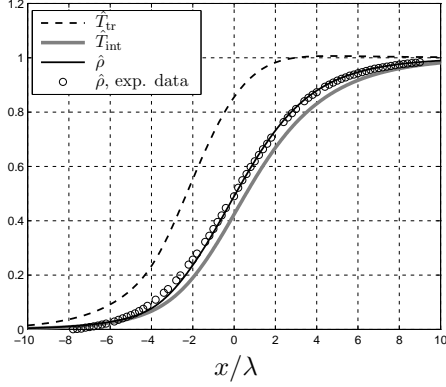
Figure 6: Comparison between monatomic and polyatomic cases.

Six Mach numbers ranging from $Ma = 1.53$ to $Ma = 6.1$ are taken into account. Similar as [9], in order to avoid the problem of hyperbolicity, only the 24 moment system ($M_0 = 3$) is used in our computation. The numerical results are plotted in Figure 7, where all macroscopic variables are normalized so that the computational results can match the data in [2]. Precisely, we use

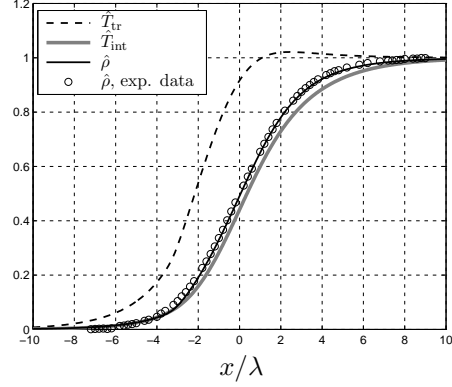
$$\hat{\rho} = \frac{\rho - \rho_l}{\rho_r - \rho_l}, \quad \hat{T}_{\text{tr}} = \frac{T_{\text{tr}} - T_l}{T_r - T_l}, \quad \hat{T}_{\text{int}} = \frac{T_{\text{int}} - T_l}{T_r - T_l}, \quad (4.9)$$

and λ denotes the mean free path. It can be found that the density profiles are in very

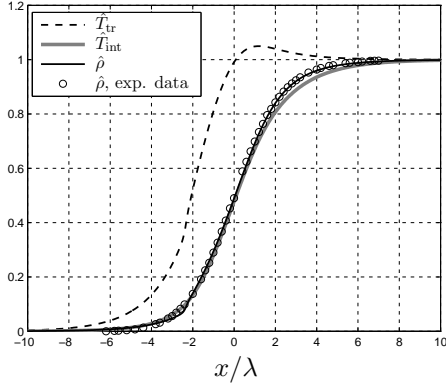
good agreements with the experimental data and no subshocks exist in the shock structure. With increasing Mach number, the numerical result gradually deviates from the experimental data. Only when Ma is as great as 6.1, the deviation in the low density region (around $x/\lambda \in (-4, -1)$ in the figure) is becoming obvious.



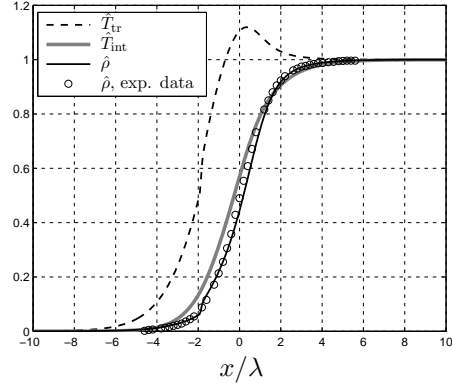
(a) $Ma = 1.53$



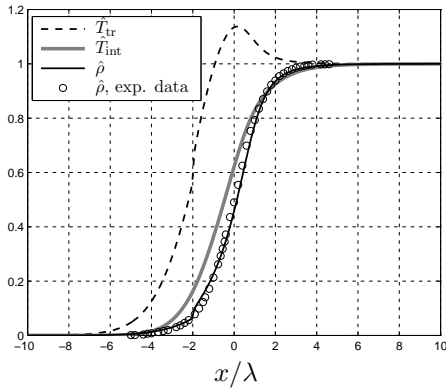
(b) $Ma = 1.7$



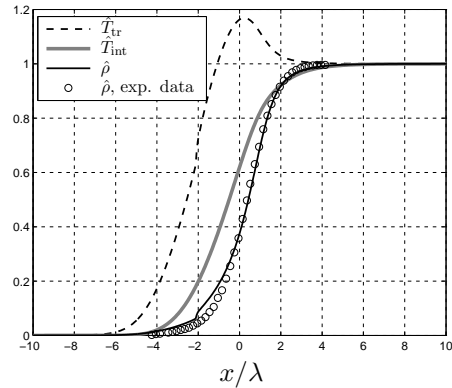
(c) $Ma = 2.0$



(d) $Ma = 3.2$



(e) $Ma = 3.8$



(f) $Ma = 6.1$

Figure 7: Structure of the nitrogen shock wave. All quantities are normalized.

5 Concluding remarks

In this paper, the NRxx method is extended to the polyatomic gases. Further investigations such as the boundary conditions and the multidimensional simulations are in progress.

Acknowledgements

This research was supported in part by the National Basic Research Program of China (2011CB309704) and Fok Ying Tong Education and NCET in China.

A Properties of Hermite and Laguerre polynomials

The Hermite polynomials defined in (3.4) are a set of orthogonal polynomials over the domain $(-\infty, +\infty)$. Below we list some of their properties which are used in this paper:

1. Orthogonality: $\int_{\mathbb{R}} He_{n_1}(x) He_{n_2}(x) \exp(-x^2/2) dx = n_1! \sqrt{2\pi} \delta_{n_1 n_2}$;
2. Recursion relation: $He_{n+1}(x) = x He_n(x) - n He_{n-1}(x)$;
3. Differential relation: $He'_n(x) = n He_{n-1}(x)$.

All these properties can be found in many mathematical handbooks such as [1]. And the following equality can be derived from the last two relations:

$$[He_n(x) \exp(-x^2/2)]' = -He_{n+1}(x) \exp(-x^2/2). \quad (\text{A.1})$$

As introduced in Section 3.1, the Laguerre polynomials defined in (3.3) are orthogonal over $[0, +\infty)$. The Laguerre polynomials are closely related to the Hermite polynomials, and they have very similar properties:

1. Orthogonality: $\int_{\mathbb{R}^+} L_{k_1}^{(m)}(x) L_{k_2}^{(m)}(x) x^m \exp(-x) dx = \gamma_{k_1}^{(m)} \delta_{k_1 k_2}$;
2. Recursion relation: $(k+1) L_{k+1}^{(m)}(x) = (m+1+k-x) L_k^{(m)}(x) - x L_{k-1}^{(m+1)}(x)$;
3. Differential relation: $[L_k^{(m)}(x)]' = -L_{k-1}^{(m+1)}(x)$.

And the last two relations give

$$[L_k^{(m)}(x) \exp(-x)]' = x^{-1} [(k+1) L_{k+1}^{(m)}(x) - (m+1+k) L_k^{(m)}(x)] \exp(-x). \quad (\text{A.2})$$

B The deduction of polyatomic moment equations

In this appendix, we are going to give the detailed deduction of (3.10). For simplicity, we define

$$\begin{aligned} \psi_{1,\alpha,T_{\text{tr}}}(\mathbf{v}) &= \left(\sqrt{2\pi}\right)^{-3} (RT_{\text{tr}})^{-\frac{|\alpha|+3}{2}} \prod_{d=1}^3 He_{\alpha_d}(v_d) \exp\left(-\frac{v_d^2}{2}\right), \\ \psi_{2,k,T_{\text{int}}}(J) &= \frac{2}{\delta} \left(\gamma_k^{(m)}\right)^{-1} (RT_{\text{int}})^{-(\delta/2+k)} L_k^{(m)}(J) \exp(-J). \end{aligned} \quad (\text{B.1})$$

Thus $\psi_{\alpha,k,T_{\text{tr}},T_{\text{int}}}(\mathbf{v}, J) = \psi_{1,\alpha,T_{\text{tr}}}(\mathbf{v})\psi_{2,k,T_{\text{int}}}(J)$. It has been deduced in [8] that

$$\frac{\partial}{\partial \eta} \psi_{1,\alpha,T_{\text{tr}}} \left(\frac{\boldsymbol{\xi} - \mathbf{u}}{\sqrt{RT_{\text{tr}}}} \right) = \sum_{d=1}^3 \left[\frac{\partial u_d}{\partial \eta} \psi_{1,\alpha+e_d,T_{\text{tr}}} \left(\frac{\boldsymbol{\xi} - \mathbf{u}}{\sqrt{RT_{\text{tr}}}} \right) + \frac{1}{2} \frac{\partial(RT_{\text{tr}})}{\partial \eta} \psi_{1,\alpha+2e_d,T_{\text{tr}}} \left(\frac{\boldsymbol{\xi} - \mathbf{u}}{\sqrt{RT_{\text{tr}}}} \right) \right], \quad (\text{B.2})$$

where η stands for t or x_j , $j = 1, 2, 3$. Now using (A.2), we have

$$\begin{aligned} & \frac{\partial}{\partial \eta} \psi_{2,k,T_{\text{int}}} \left(\frac{I^{2/\delta}}{RT_{\text{int}}} \right) \\ &= -\frac{2}{\delta} \left(\gamma_k^{(m)} \right)^{-1} \left(\frac{\delta}{2} + k \right) (RT_{\text{int}})^{-(\delta/2+k+1)} \frac{\partial(RT_{\text{int}})}{\partial \eta} L_k^{(m)} \left(\frac{I^{2/\delta}}{RT_{\text{int}}} \right) \exp \left(-\frac{I^{2/\delta}}{RT_{\text{int}}} \right) \\ &+ \frac{2}{\delta} \left(\gamma_k^{(m)} \right)^{-1} (RT_{\text{int}})^{-(\delta/2+k)} \frac{RT_{\text{int}}}{I^{2/\delta}} \frac{\partial}{\partial \eta} \left(\frac{I^{2/\delta}}{RT_{\text{int}}} \right) \exp \left(-\frac{I^{2/\delta}}{RT_{\text{int}}} \right) \times \\ & \left[(k+1) L_{k+1}^{(m)} \left(\frac{I^{2/\delta}}{RT_{\text{int}}} \right) - (m+1+k) L_k^{(m)} \left(\frac{I^{2/\delta}}{RT_{\text{int}}} \right) \right]. \end{aligned} \quad (\text{B.3})$$

Since $m = \delta/2 - 1$ and

$$\frac{RT_{\text{int}}}{I^{2/\delta}} \frac{\partial}{\partial \eta} \left(\frac{I^{2/\delta}}{RT_{\text{int}}} \right) = -\frac{1}{RT_{\text{int}}} \frac{\partial(RT_{\text{int}})}{\partial \eta}, \quad (\text{B.4})$$

the equation (B.3) can be simplified as

$$\begin{aligned} & \frac{\partial}{\partial \eta} \psi_{2,k,T_{\text{int}}} \left(\frac{I^{2/\delta}}{RT_{\text{int}}} \right) \\ &= -\frac{2}{\delta} \left(\gamma_k^{(m)} \right)^{-1} (k+1) (RT_{\text{int}})^{-(\delta/2+k+1)} \frac{\partial(RT_{\text{int}})}{\partial \eta} L_{k+1}^{(m)} \left(\frac{I^{2/\delta}}{RT_{\text{int}}} \right) \exp \left(-\frac{I^{2/\delta}}{RT_{\text{int}}} \right). \end{aligned} \quad (\text{B.5})$$

Noting that

$$\frac{\gamma_{k+1}^{(m)}}{\gamma_k^{(m)}} = \frac{\Gamma(m+k+2)}{\Gamma(m+k+1)} \cdot \frac{\Gamma(k+1)}{\Gamma(k+2)} = \frac{m+k+1}{k+1}, \quad (\text{B.6})$$

one finally obtains a simple expression:

$$\frac{\partial}{\partial \eta} \psi_{2,k,T_{\text{int}}} \left(\frac{I^{2/\delta}}{RT_{\text{int}}} \right) = -(m+k+1) \psi_{2,k+1,T_{\text{int}}} \left(\frac{I^{2/\delta}}{RT_{\text{int}}} \right). \quad (\text{B.7})$$

Thus the derivative of the basis function (3.1) is

$$\begin{aligned} \frac{\partial}{\partial \eta} \psi_{\alpha,k,T_{\text{tr}},T_{\text{int}}} &= -(m+k+1) \psi_{\alpha,k+1,T_{\text{tr}},T_{\text{int}}} \\ &+ \sum_{d=1}^3 \left[\frac{\partial u_d}{\partial \eta} \psi_{\alpha+e_d,k,T_{\text{tr}},T_{\text{int}}} + \frac{1}{2} \frac{\partial(RT_{\text{tr}})}{\partial \eta} \psi_{\alpha+2e_d,k,T_{\text{tr}},T_{\text{int}}} \right]. \end{aligned} \quad (\text{B.8})$$

Here $\psi_{\alpha,k,T_{\text{tr}},T_{\text{int}}}$ stands for

$$\psi_{\alpha,k,T_{\text{tr}},T_{\text{int}}} \left(\frac{\boldsymbol{\xi} - \mathbf{u}}{\sqrt{RT_{\text{tr}}}}, \frac{I^{2/\delta}}{RT_{\text{int}}} \right). \quad (\text{B.9})$$

The parameters are omitted for conciseness.

Now we expand the left hand side of (2.1) into series. Using (B.8), one immediately has

$$\begin{aligned} \frac{\partial f}{\partial t} &= \sum_{\alpha \in \mathbb{N}^3} \sum_{k \in \mathbb{N}} \left[\frac{\partial f_{\alpha,k}}{\partial t} \psi_{\alpha,k,T_{\text{tr}},T_{\text{int}}} + f_{\alpha,k} \frac{\partial}{\partial t} \psi_{\alpha,k,T_{\text{tr}},T_{\text{int}}} \right] \\ &= \sum_{\alpha \in \mathbb{N}^3} \sum_{k \in \mathbb{N}} \left[\frac{\partial f_{\alpha,k}}{\partial t} + \sum_{d=1}^3 \frac{\partial u_d}{\partial t} f_{\alpha+e_d,k} \right. \\ &\quad \left. + \frac{1}{2} \frac{\partial(RT_{\text{tr}})}{\partial t} \sum_{d=1}^3 f_{\alpha-2e_d,k} - (m+k) \frac{\partial(RT_{\text{int}})}{\partial t} f_{\alpha,k-1} \right] \psi_{\alpha,k,T_{\text{tr}},T_{\text{int}}}. \end{aligned} \quad (\text{B.10})$$

For the convection term, we have

$$\begin{aligned} \boldsymbol{\xi} \cdot \nabla_{\mathbf{x}} f &= \sum_{j=1}^3 \xi_j \frac{\partial f}{\partial x_j} = \sum_{j=1}^3 \xi_j \sum_{\alpha \in \mathbb{N}^3} \sum_{k \in \mathbb{N}} \left[\frac{\partial f_{\alpha,k}}{\partial x_j} + \sum_{d=1}^3 \frac{\partial u_d}{\partial x_j} f_{\alpha+e_d,k} \right. \\ &\quad \left. + \frac{1}{2} \frac{\partial(RT_{\text{tr}})}{\partial x_j} \sum_{d=1}^3 f_{\alpha-2e_d,k} - (m+k) \frac{\partial(RT_{\text{int}})}{\partial x_j} f_{\alpha,k-1} \right] \psi_{\alpha,k,T_{\text{tr}},T_{\text{int}}}. \end{aligned} \quad (\text{B.11})$$

Now we use (3.73) and get

$$\begin{aligned} \boldsymbol{\xi} \cdot \nabla_{\mathbf{x}} f &= \sum_{\alpha \in \mathbb{N}^3} \sum_{k \in \mathbb{N}} \sum_{j=1}^3 \left[\left(RT_{\text{tr}} \frac{\partial f_{\alpha-e_j,k}}{\partial x_j} + u_j \frac{\partial f_{\alpha,k}}{\partial x_j} + (\alpha_j + 1) \frac{\partial f_{\alpha+e_j,k}}{\partial x_j} \right) \right. \\ &\quad + \sum_{d=1}^3 \frac{\partial u_d}{\partial x_j} (RT_{\text{tr}} f_{\alpha-e_d-e_j,k} + u_j f_{\alpha-e_d,k} + (\alpha_j + 1) f_{\alpha-e_d+e_j,k}) \\ &\quad + \frac{1}{2} \frac{\partial(RT_{\text{tr}})}{\partial x_j} \sum_{d=1}^3 (RT_{\text{tr}} f_{\alpha-2e_d-e_j,k} + u_j f_{\alpha-2e_d,k} + (\alpha_j + 1) f_{\alpha-2e_d+e_j,k}) \\ &\quad \left. - (m+k) \frac{\partial(RT_{\text{int}})}{\partial x_j} (RT_{\text{tr}} f_{\alpha-e_j,k-1} + u_j f_{\alpha,k-1} + (\alpha_j + 1) f_{\alpha+e_j,k-1}) \right] \psi_{\alpha,k,T_{\text{tr}},T_{\text{int}}}. \end{aligned} \quad (\text{B.12})$$

Collecting (B.10)(B.12) and (3.9), the moment system (3.10) follows naturally.

C Expansion of the generalized Gaussian

This section is devoted to the calculation of $G_{\alpha,0}$, which is defined in (3.9). In this appendix, G is considered as a function of $\boldsymbol{\xi}$ and I , where the parameters t and \mathbf{x} are

omitted. It can be deduced from the orthogonality of Hermite and Laguerre polynomials that

$$G_{\alpha,0} = C_{\alpha,T_{\text{tr}}} \int_{\mathbb{R}^3 \times \mathbb{R}^+} p_{\alpha,T_{\text{tr}}}(\mathbf{v}) G(\mathbf{u} + \sqrt{RT_{\text{tr}}}\mathbf{v}, I) d\mathbf{v} dI, \quad (\text{C.1})$$

where $p_{\alpha,T_{\text{tr}}}$ is a polynomial defined as

$$p_{\alpha,T_{\text{tr}}}(\mathbf{v}) = \psi_{1,\alpha,T_{\text{tr}}}(\mathbf{v}) \exp\left(-\frac{|\mathbf{v}|^2}{2}\right) = \left(\sqrt{2\pi}\right)^{-3} (RT_{\text{tr}})^{-\frac{|\alpha|+3}{2}} \prod_{d=1}^3 He_{\alpha_d}(v_d), \quad (\text{C.2})$$

and $C_{\alpha,T_{\text{tr}}}$ is a constant dependent on α and T_{tr} :

$$C_{\alpha,T_{\text{tr}}} = \frac{(2\pi)^{-\frac{3}{2}} (RT_{\text{tr}})^{3+|\alpha|}}{\alpha_1! \alpha_2! \alpha_3!}. \quad (\text{C.3})$$

For $i \in \{1, 2, 3\}$, if $\alpha_i > 0$, the recursion relation of Hermite polynomials shows that

$$p_{\alpha,T_{\text{tr}}}(\mathbf{v}) = (RT_{\text{tr}})^{-\frac{1}{2}} v_i p_{\alpha-e_i,T_{\text{tr}}}(\mathbf{v}) - (RT_{\text{tr}})^{-1} (\alpha_i - 1) p_{\alpha-2e_i,T_{\text{tr}}}(\mathbf{v}). \quad (\text{C.4})$$

Noting that

$$C_{\alpha,T_{\text{tr}}} = \frac{(RT_{\text{tr}})^2}{\alpha_i(\alpha_i - \delta_{ik})} C_{\alpha-e_i-e_k,T_{\text{tr}}} = \frac{(RT_{\text{tr}})^2}{\alpha_i(\alpha_i - 1)} C_{\alpha-2e_i,T_{\text{tr}}}, \quad (\text{C.5})$$

one directly obtains from (C.1) that

$$G_{\alpha,0} = C_{\alpha,T_{\text{tr}}} (RT_{\text{tr}})^{-\frac{1}{2}} \int_{\mathbb{R}^3 \times \mathbb{R}^+} v_i p_{\alpha-e_i,T_{\text{tr}}}(\mathbf{v}) G(\mathbf{u} + \sqrt{RT_{\text{tr}}}\mathbf{v}, I) d\mathbf{v} dI - \frac{RT_{\text{tr}}}{\alpha_i} G_{\alpha-2e_i,0}. \quad (\text{C.6})$$

Now the expression of G (2.2) is put into the above equation. After integrating with respect to I , one has

$$G_{\alpha,0} = \frac{C_{\alpha,T_{\text{tr}}} \rho (RT_{\text{tr}})^{-\frac{1}{2}}}{\sqrt{\det(2\pi\mathcal{T})}} \int_{\mathbb{R}^3} v_i p_{\alpha-e_i,T_{\text{tr}}}(\mathbf{v}) \exp\left(-\frac{RT_{\text{tr}}}{2} \mathbf{v}^T \mathcal{T}^{-1} \mathbf{v}\right) d\mathbf{v} - \frac{RT_{\text{tr}}}{\alpha_i} G_{\alpha-2e_i,0}. \quad (\text{C.7})$$

The matrix \mathcal{T} is required to be positive definite, since the density of the fluid should be finite. Thus, there exists a matrix $\mathcal{R} = (r_{ij})$ such that $\mathcal{T} = (RT_{\text{tr}}) \mathcal{R} \mathcal{R}^T$. Making the transformation $\mathbf{w} = \mathcal{R}^{-1} \mathbf{v}$, and noting that $\det(\mathcal{T}) = (RT_{\text{tr}})^3 [\det(\mathcal{R})]^2$, (C.7) becomes

$$G_{\alpha,0} = \frac{C_{\alpha,T_{\text{tr}}} \rho}{(\sqrt{2\pi})^3 (RT_{\text{tr}})^2} \sum_{j=1}^3 r_{ij} \int_{\mathbb{R}^3} w_j p_{\alpha-e_i,T_{\text{tr}}}(\mathcal{R}\mathbf{w}) \exp(-|\mathbf{w}|^2/2) d\mathbf{w} - \frac{RT_{\text{tr}}}{\alpha_i} G_{\alpha-2e_i,0}. \quad (\text{C.8})$$

The following relation is a direct result of the differential relation of Hermite polynomials:

$$\frac{\partial}{\partial w_j} p_{\alpha,T_{\text{tr}}}(\mathcal{R}\mathbf{w}) = (RT_{\text{tr}})^{-\frac{1}{2}} \sum_{k=1}^3 \alpha_k r_{kj} p_{\alpha-e_k,T_{\text{tr}}}(\mathcal{R}\mathbf{w}). \quad (\text{C.9})$$

Thus it can be obtained by integrating by parts that

$$\begin{aligned} & \int_{\mathbb{R}^3} w_j p_{\alpha-e_i,T_{\text{tr}}}(\mathcal{R}\mathbf{w}) \exp(-|\mathbf{w}|^2/2) d\mathbf{w} \\ &= (RT_{\text{tr}})^{-\frac{1}{2}} \sum_{k=1}^3 (\alpha_k - \delta_{ik}) r_{kj} \int_{\mathbb{R}^3} p_{\alpha-e_i-e_k,T_{\text{tr}}}(\mathcal{R}\mathbf{w}) \exp(-|\mathbf{w}|^2/2) d\mathbf{w}. \end{aligned} \quad (\text{C.10})$$

Now we substitute (C.10) into (C.8), and apply the transformation $\mathbf{v} = \mathcal{R}\mathbf{w}$. The result is

$$G_{\alpha,0} = \frac{\rho}{\sqrt{\det(2\pi\mathcal{T})}} \sum_{j=1}^3 r_{ij} \sum_{k=1}^3 r_{kj} \cdot \frac{C_{\alpha,T_{\text{tr}}}(\alpha_k - \delta_{ik})}{RT_{\text{tr}}} \times \int_{\mathbb{R}^3} p_{\alpha-e_i-e_k,T_{\text{tr}}}(\mathbf{v}) \exp\left(-\frac{RT_{\text{tr}}}{2} \mathbf{v}^T \mathcal{T}^{-1} \mathbf{v}\right) d\mathbf{v} - \frac{RT_{\text{tr}}}{\alpha_i} G_{\alpha-2e_i,0}. \quad (\text{C.11})$$

Using (C.5), it is not difficult to find

$$G_{\alpha,0} = \frac{RT_{\text{tr}}}{\alpha_i} \left(\sum_{j=1}^3 r_{ij} \sum_{k=1}^3 r_{kj} G_{\alpha-e_i-e_k} - G_{\alpha-2e_i,0} \right). \quad (\text{C.12})$$

Recalling $\mathcal{T} = (RT_{\text{tr}})\mathcal{R}\mathcal{R}^T$, the above equation can be written as

$$G_{\alpha,0} = \frac{1}{\alpha_i} \sum_{k=1}^3 (\lambda_{ik} - RT_{\text{tr}}\delta_{ik}) G_{\alpha-e_i-e_k,0}, \quad (\text{C.13})$$

where λ_{ik} is the (i,k) -element of \mathcal{T} . The final result (3.17) is then obtained by substituting the detailed expression of \mathcal{T} into (C.13).

References

- [1] M. Abramowitz and I. A. Stegun. *Handbook of Mathematical Functions with Formulas, Graphs, and Mathematical Tables*. Dover, New York, 1964.
- [2] H. Alsmeyer. Density profiles in argon and nitrogen shock waves measured by the absorption of an electron beam. *J. Fluid. Mech.*, 74(3):497–513, 1976.
- [3] P. Andries, J. F. Bourgat, P. L. Tallec, and B. Perthame. Numerical comparison between the Boltzmann and ES-BGK models for rarefied gases. *Comput. Methods Appl. Mech. Engrg.*, 191(31):3369–3390, 2002.
- [4] P. Andries, P. L. Tallec, J. P. Perlat, and B. Perthame. The Gaussian-BGK model of Boltzmann equation with small Prandtl number. *Eur. J. Mech. B - Fluids*, 19(6):813–830, 2000.
- [5] J. D. Au, M. Torrilhon, and W. Weiss. The shock tube study in extended thermodynamics. *Phys. Fluids*, 13(8):2423–2432, 2001.
- [6] S. Brull and J. Schneider. On the ellipsoidal statistical model for polyatomic gases. *Continuum Mech. Thermodyn.*, 20(8):489–508, 2009.
- [7] Z. Cai and R. Li. Numerical regularized moment method of arbitrary order for Boltzmann-BGK equation. *SIAM J. Sci. Comput.*, 32(5):2875–2907, 2010.
- [8] Z. Cai, R. Li, and Y. Wang. An efficient NRxx method for Boltzmann-BGK equation. *J. Sci. Comput.*, 50(1):103–119, 2012.
- [9] Z. Cai, R. Li, and Y. Wang. Numerical regularized moment method for high Mach number flow. *Commun. Comput. Phys.*, 11(5):1415–1438, 2012.

- [10] B. Dubroca and L. Mieussens. A conservative and entropic discrete-velocity model for rarefied polyatomic gases. In *CEMRACS 1999 (Orsay)*, volume 10 of *ESAIM Proc.*, pages 127–139, Paris, 1999. Soc. Math. Appl. Indust.
- [11] H. Grad. On the kinetic theory of rarefied gases. *Comm. Pure Appl. Math.*, 2(4):331–407, 1949.
- [12] H. Grad. The profile of a steady plane shock wave. *Comm. Pure Appl. Math.*, 5(3):257–300, 1952.
- [13] I. N. Larina and V. A. Rykov. Kinetic model of the Boltzmann equation for a diatomic gas with rotational degrees of freedom. *Comput. Math. Math. Phys.*, 50(12):2118–2130, 2010.
- [14] F. Mallinger. Generalization of the Grad theory to polyatomic gases. Rapport de recherche 3581, INRIA Rocquencourt, 1998.
- [15] F. J. McCormack. Kinetic equations for polyatomic gases: The 17-moment approximation. *Phys. Fluids*, 11(12):2533–2543, 1968.
- [16] L. Mieussens. Discrete velocity model and implicit scheme for the BGK equation of rarefied gas dynamics. *Math. Models Methods Appl. Sci.*, 10(8):1121–1149, 2000.
- [17] I. Müller, D. Reitebuch, and W. Weiss. Extended thermodynamics – consistent in order of magnitude. *Continuum Mech. Thermodyn.*, 15(2):113–146, 2002.
- [18] V. A. Rykov. A model kinetic equation for a gas with rotational degrees of freedom. *Fluid Dyn.*, 10(6):959–966, 1975.
- [19] H. Struchtrup. Stable transport equations for rarefied gases at high orders in the Knudsen number. *Phys. Fluids*, 16(11):3921–3934, 2004.
- [20] H. Struchtrup. *Macroscopic Transport Equations for Rarefied Gas Flows: Approximation Methods in Kinetic Theory*. Springer, 2005.
- [21] H. Struchtrup and M. Torrilhon. Regularization of Grad’s 13 moment equations: Derivation and linear analysis. *Phys. Fluids*, 15(9):2668–2680, 2003.
- [22] M. Torrilhon. Characteristic waves and dissipation in the 13-moment-case. *Continuum Mech. Thermodyn.*, 12(5):289–301, 2000.
- [23] M. Torrilhon, J. Au, D. Reitebuch, and W. Weiss. The Riemann-problem in extended thermodynamics. In H. Freistühler and G. Warnecke, editors, *Hyperbolic Problems: Theory, Numerics, Applications, Vols I and II*, volume 140 of *International series of numerical mathematics*, pages 79–88. Birkhäuser, 2001.
- [24] K. Xu and L. Tang. Nonequilibrium Bhatnagar-Gross-Krook model for nitrogen shock structure. *Phys. Fluids*, 16(10):3824–3827, 2004.